Supplementary Information (SI) for Green Chemistry.
This journal is © The Royal Society of Chemistry 2026

Supplementary material

Catalyst-free polyesterification enables multifunctional and sustainable polyester

Hongjie Zhang,[*‡a] Miaomiao Wang,[‡a] Shihao Niu,[a] Qiuquan Cai,[*b] Wenxing Chen,[a] Wangyang Lu[*a]

[a]State Key Laboratory of Bio-based Fiber Materials, Zhejiang Sci-Tech University, Hangzhou 310018, China

[b]Innovation Center for Textile Materials, Chemistry and Chemical Engineering Guangdong Laboratory, Shantou 515031, China

[*]Correspondence: zhanghj@zstu.edu.cn (Hongjie Zhang); caiqq@ccelab.com.cn (Qiuquan Cai); luwy@zstu.edu.cn (Wangyang Lu)

Contents

1. Materials

Succinic acid (SA), ethylene glycol (EG), and sodium 3,5-dicarboxybenzenesulfonate (NaSIPA) were purchased from Aladdin Biochemical Technology Co., Ltd. Hexafluoroisopropanol (HFIP) was purchased from Macklin Biochemical Co., Ltd. Chloroform and dimethyl sulfoxide-d6 (DMSO) were purchased from Hangzhou Gaojingchem Co., Ltd. *N*,*N*,*N*-trimethyl-1-tetradecanammonium bromide (Cetrimide) were purchased from Shanghai Acmec Biochemical Technology Co., Ltd. All reagents and solvents were of analytical grade and were used as received.

2. Experimental method

All operations for the synthesis of multifunctional copolyesters were carried out in 250 mL three-necked round-bottom flasks equipped with a mechanically magnetic stirrer. In the initial stage, under an argon atmosphere, EG, SA, and NaSIPA were sequentially added to a flask at varying molar ratios. The temperature was subsequently increased to a range of 130-180 °C to promote polyesterification, allowing the reaction to reach completion and leading to the formation of carboxy-terminated prepolymer. In the second stage, the three-necked flask were connected to an oil pump to ensure that the vacuum pressure within the polymerization system remained below 100 Pa. Subsequently, the temperature was incrementally increased to 240 °C. The polycondensation should proceed until the viscosity reaches a maximum and no longer increases. Under conditions of elevated temperature and reduced pressure, anhydride was continuously removed from the polymerization system via sublimation, leading to a continuous increase in viscosity and ultimately yielding a high molecular weight copolyester.

3. Electrospinning

PESSIPA0.1 was dissolved in hexafluoroisopropanol to achieve a mass fraction of 5%. Subsequently, the solution was transferred into the reservoir of the spinning apparatus, which was

equipped with a spinneret. The absorber surface was covered with a sheet of aluminum foil, after which the chamber door was closed. The voltage was set to 10 kV and the rotational speed to 3000 rpm. Following a 2-minute interval, the rotational speed and voltage were gradually reduced to zero before removing the aluminum foil. Finally, a small section of the sample was excised for examination under a scanning electron microscope (SEM, Hitachi Regulus8100).

4. Characterizations

Proton (^{1}H) and carbon (^{13}C) nuclear magnetic resonance (NMR)

^{1}H and ^{13}C NMR spectroscopy were determined using a Bruker Avance III HD 400 MHz spectrometer (German). Chemical shift value was based on tetramethylsilane (TMS) at 0 ppm as a reference. Typically, chloroform or dimethyl sulfoxide (DMSO) served as the deuterated solvent.

Absolute molecular weight

The absolute molecular weight of the sample was measured by ultra-high performance polymer chromatography-multi-angle laser light scattering detector-differential detector (APC-MALLS-RID) detection technology. The detection technology can combine the advantages of chromatography and light scattering method. When the solution flows through the chromatographic column, it is eluted and separated according to the order of molecular size from large to small, and then the response signal is generated by MALLS and RID, which can quickly and accurately detect M_n and M_w. The mobile phase consisted of a solution of hexafluoroisopropanol (HFIP) and sodium trifluoroacetate, prepared by dissolving 680 mg of sodium trifluoroacetate in 1000 ml of HFIP. The sample concentration was maintained at 2 mg·ml^{-1}, and the flow rate of the mobile phase was set to 0.4 ml·min^{-1} during the analysis.

Attenuated total reflectance-Fourier transform infrared (ATR-FTIR)

ATR-FTIR spectra were obtained by an INVENIO R spectrophotometer. In order to facilitate the measurement, the samples were compressed into thin sheets with smooth surface to testing.

X-ray photoelectron spectroscopy (XPS)

XPS was performed using the Thermo Scientific ESCALAB 250 Xi instrument.

X-Ray Diffraction (XRD)

X-ray diffraction (XRD) was performed using a D8 discover X-ray diffractometer. All samples were thin films with a thickness of 0.5 mm.

Tensile test

The tensile test used the tensile testing machine of Dongguan Dongri Instrument Co., Ltd. Specimens with a dumbbell shape, in accordance with the ASTM D638-14 standard, were utilized for the tensile tests. The testing was conducted at a speed of 50 $mm \cdot min^{-1}$.

Thermogravimetric analysis (TGA)

The samples were analyzed using a Mettler-Toledo TGA instrument (Switzerland). Each sample, with a mass of approximately 5-8 mg, was heated from 50 to 600 °C at a heating rate of 10 $°C \cdot min^{-1}$ under a nitrogen flow of 50 $mL \cdot min^{-1}$. The temperature corresponding to 10% mass loss ($T_{d,10\%}$) was determined based on the recorded thermogravimetric curve.

Differential scanning calorimetry (DSC)

The samples were analyzed using a Mettler Toledo DSC1 instrument (Switzerland) under a nitrogen atmosphere. In order to eliminate the thermal history effect, the samples (5-8 mg) were heated from 25 to 280 °C at a rate of 10 $°C \cdot min^{-1}$ and kept at the final temperature for 3 min. The samples were then cooled to -50 °C at a rate of 5 $°C \cdot min^{-1}$ and finally raised to 280 °C at a rate of 10 $°C \cdot min^{-1}$ to determine the glass transition temperature (T_g) and melting point (T_m), respectively.

Dynamic mechanical analysis (DMA)

DMA tests were conducted using the METTLER TDMA1 instrument, with samples prepared in the form of rectangular splines measuring 4 mm in width, 2 mm in thickness, and 15 mm in length. The DMA investigations were conducted over a temperature range of -30 to 90 °C, utilizing a heating rate of 5 °C·min^{-1} in extension mode with a sinusoidal stress frequency of 1 Hz. The storage modulus (E'), loss modulus (E''), and loss factor (tan δ) were systematically monitored as functions of temperature. The glass transition temperature (T_g) was determined as the point of the inflection on the loss modulus curve (E'') according to ISO6721-11:2019.

Small-angel X-ray scattering (SAXS)

The Xeuss 2.0 small-angle X-ray scattering (SAXS) instrument, manufactured by Xenocs in France, was utilized for this study. The X-ray wavelength employed was 1.54189 Å. The sample, a rectangular spline with a thickness of 1 mm, was positioned at a distance of 1188 mm from the detector. Two-dimensional SAXS patterns were captured using a Pilatus 3R 300K semiconductor detector.

Transmission electron microscope (TEM)

The morphology of the samples was observed by JEM-1400 flash transmission electron microscope, and the acceleration voltage was 40 kV-120 kV. A sample solution with a concentration of 1mg·mL^{-1} was carefully deposited onto the copper grid, followed by drying under an infrared lamp. Subsequently, the morphological characteristics of the cationic aggregates were examined.

Transmittance test

The transmittance of the samples was measured by Hitachi ultraviolet visible near infrared spectrophotometer UH4150. The thickness of the samples was 0.3 mm. The transmittance of the samples was measured and compared across various cooling times.

Matrix-assisted laser desorption/ionization time-of-flight mass spectrometry (MALDI- TOF-MS)

MALDI-TOF-MS analysis was performed using a Bruker Ultraflextreme MALDI-TOF mass spectrometer in positive ion mode. The matrix employed was 2,5-dihydroxybenzoic acid (DHB). The analyzer was used at an acceleration voltage +20 Kv. Laser light was focused on the sample using the 8.02 Kv lens. A pulsed ion extraction was optimized to 170 ns. For each sample, MALDI-TOF-MS was ensured on 10 distinct sample deposit zones. A total of 500 shots were provided.

Scanning electron microscope (SEM)

The morphology of the brittle fracture section of PESSIPA0.1 was observed by SEM (Thermo scientific Verios 5 UC). The initial sample was two splines with a width of 8 mm and a thickness of 1mm. After treatment, one of them was cut and welded together at room temperature and brittle fracture in liquid nitrogen, and the other was conventional brittle fracture.

Degradation experiment

The degradation of aliphatic polyesters, particularly PES, has been extensively investigated, and aliphatic polyesters is generally acknowledged as a biodegradable polymer[1-3]. However, it has been reported that the degradation rate in seawater is relatively slow[4, 5]. This study further compares the degradation rates of PES and PESSIPAs in various media to investigate the impact of NaSIPA incorporation on the degradation process. The polyesters were subjected to degradation experiments in three distinct aqueous environments under controlled conditions. The water media utilized in this study comprised seawater, PBS buffer solution, and deionized water. During the

experiment, the samples were collected regularly to observe the changes of surface morphology and record the quality changes. The morphological characteristics of polyesters following degradation in three distinct aqueous environments were examined using SEM.

Recycling and upcycling

Recycling: Dissolve the mixed plastic containing the polyester synthesized in this work in deionized water. Stir the mixture at room temperature using a magnetic stirrer operating at 500 rpm to facilitate complete dissolution. After an hour, filter the solution to remove any insoluble residues and collect the filtrate. If desired, proceed with the optional depolymerization step by heating the solution to 80 °C under continuous stirring for 2 hours, during which the polymer will be quickly converted into prepolymers. Finally, remove the water through vacuum evaporation to obtain the solid product.

Upcycling: Dissolve 5 g of PESSIPA0.1 in 10 mL either water or hexafluoroisopropanol. Once fully dissolved, add N,N,N-trimethyl-1-tetradecanammonium bromide (Cetrimide) in amounts equivalent to 0.5%, 1%, 2%, and 4% of the molar quantity of sodium sulfonate present in the PESSIPA0.1. After complete mixing, filter the solution and subsequently perform rotary evaporation to remove the solvent, thereby obtaining the product following ion substitution.

Theoretical calculation

All calculations were carried out using the Gaussian 09 program. In the exploration of reaction pathways, the M06-2X/6-311++G(d,p) method was employed to optimize the geometries of all intermediates and transition states (TSs). Frequency calculations were performed to confirm that the intermediates had no imaginary frequencies, while each TS exhibited one imaginary frequency. The intrinsic reaction coordinate (IRC) analysis was conducted to verify the reaction pathway associated with each TS. In the exploration of the structural optimization of sulfonic acid sodium

complexes, the M06-2X/6-311++G(d,p) method was utilized for geometry optimization. Frequency calculations were subsequently carried out to confirm that the optimized structure possessed no imaginary frequencies or those with values less than 30 cm^{-1}. Furthermore, the single-point energies derived from the optimized structures were corrected using a frequency scale factor of 0.9700, as implemented in Shermo 2.6[6].

Gaussian 09, Revision D.01, M. J. Frisch, G. W. Trucks, H. B. Schlegel, G. E. Scuseria, M. A. Robb, J. R. Cheeseman, G. Scalmani, V. Barone, B. Mennucci, G. A. Petersson, H. Nakatsuji, M. Caricato, X. Li, H. P. Hratchian, A. F. Izmaylov, J. Bloino, G. Zheng, J. L. Sonnenberg, M. Hada, M. Ehara, K. Toyota, R. Fukuda, J. Hasegawa, M. Ishida, T. Nakajima, Y. Honda, O. Kitao, H. Nakai, T. Vreven, J. A. Montgomery, Jr., J. E. Peralta, F. Ogliaro, M. Bearpark, J. J. Heyd, E. Brothers, K. N. Kudin, V. N. Staroverov, T. Keith, R. Kobayashi, J. Normand, K. Raghavachari, A. Rendell, J. C. Burant, S. S. Iyengar, J. Tomasi, M. Cossi, N. Rega, J. M. Millam, M. Klene, J. E. Knox, J. B. Cross, V. Bakken, C. Adamo, J. Jaramillo, R. Gomperts, R. E. Stratmann, O. Yazyev, A. J. Austin, R. Cammi, C. Pomelli, J. W. Ochterski, R. L. Martin, K. Morokuma, V. G. Zakrzewski, G. A. Voth, P. Salvador, J. J. Dannenberg, S. Dapprich, A. D. Daniels, O. Farkas, J. B. Foresman, J. V. Ortiz, J. Cioslowski, and D. J. Fox, Gaussian, Inc., Wallingford CT, 2013.

5. Figures

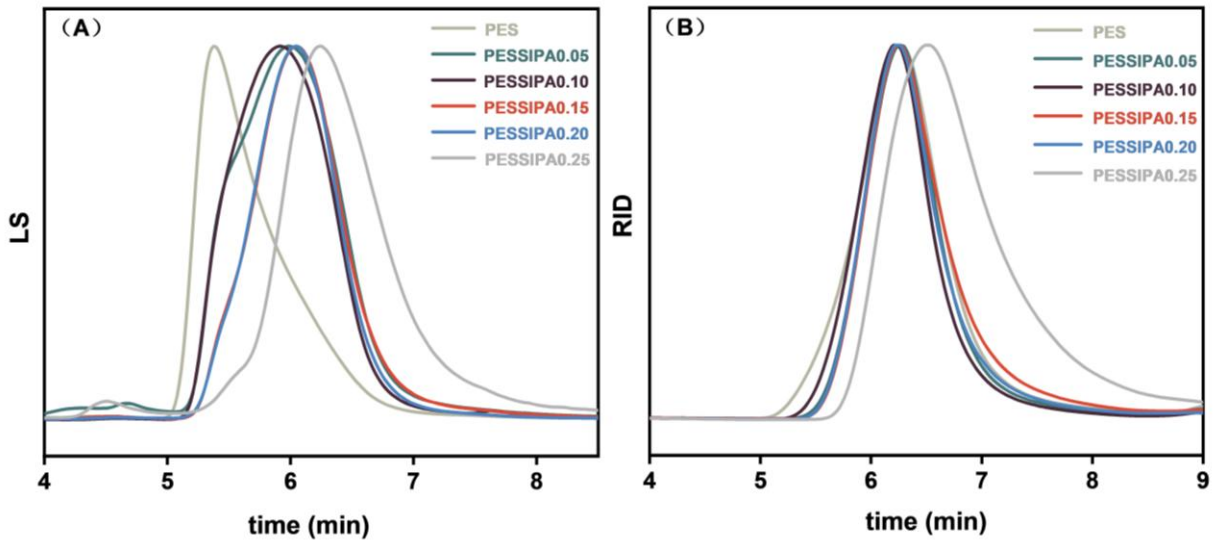

Figure S1. APC-MALLS-RID spectra of products. (A) MALLS spectra; (B) RID spectra.

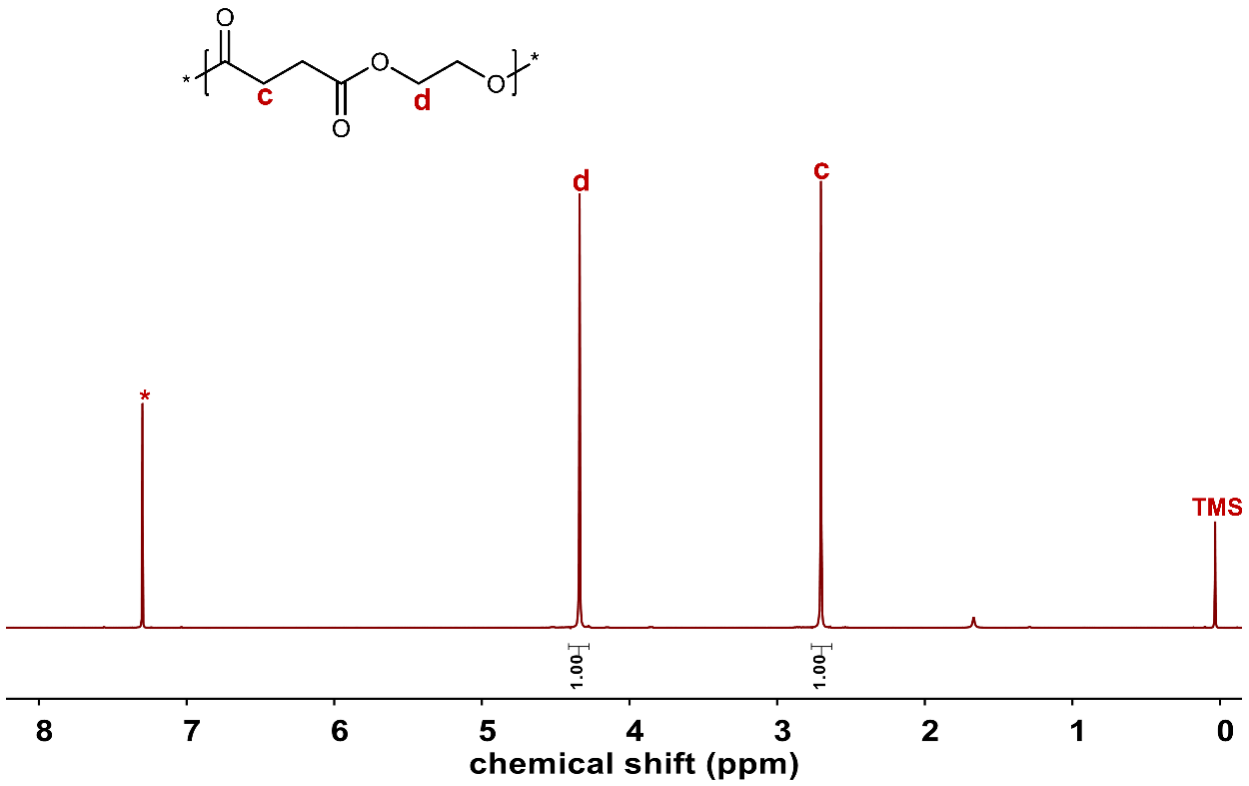

Figure S2. ^{1}H NMR spectrum of PES.

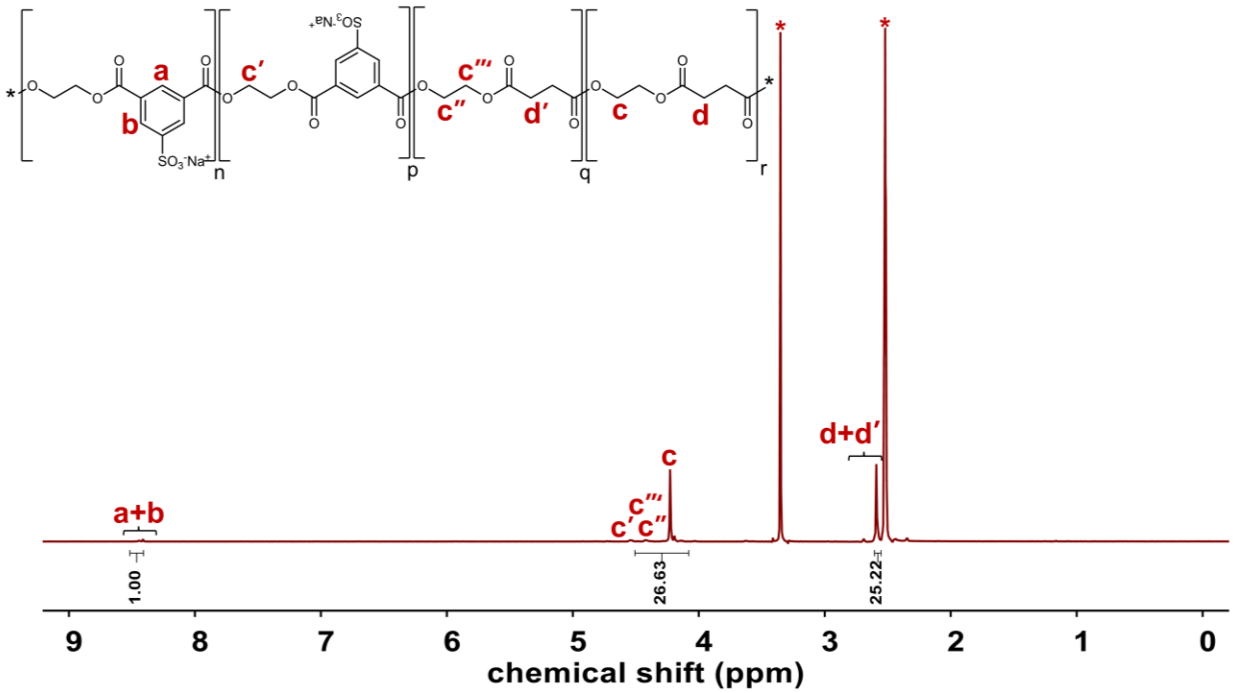

Figure S3. ^{1}H NMR spectrum of PESSIPA0.05.

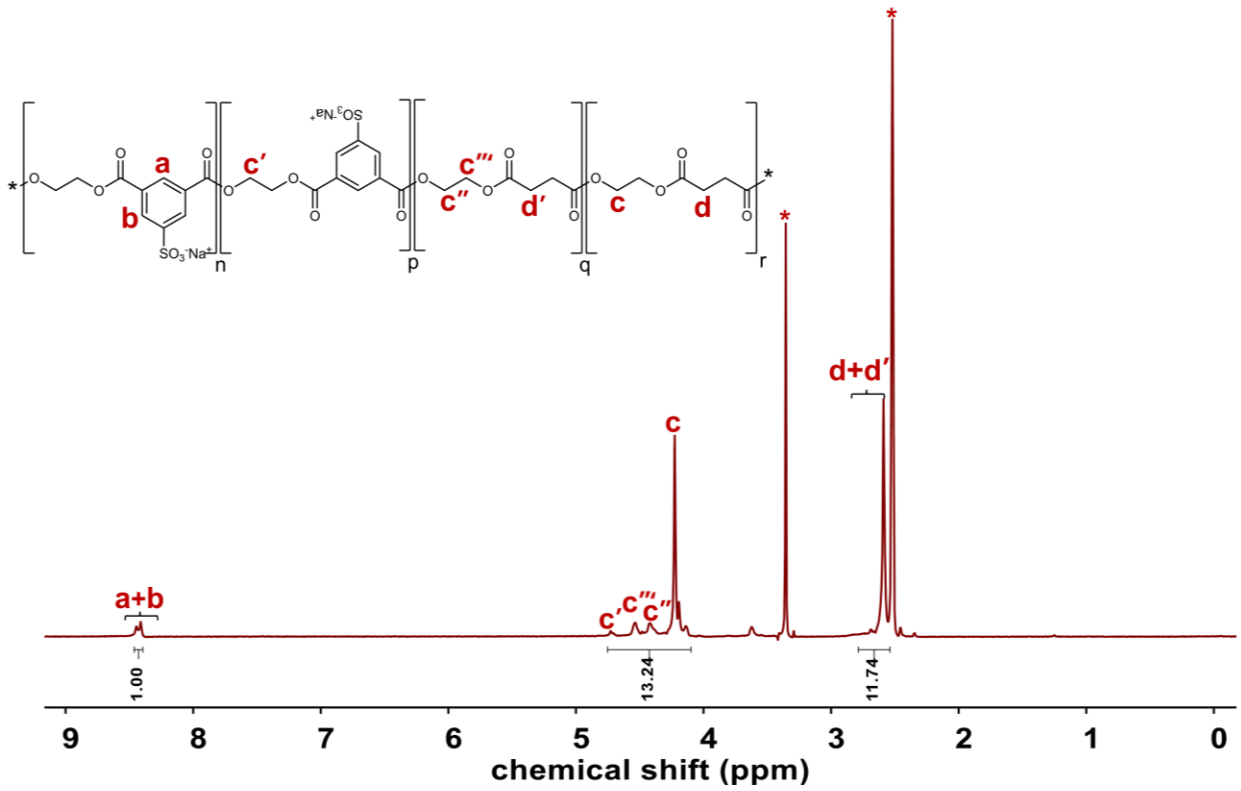

Figure S4. ^{1}H NMR spectrum of PESSIPA0.10.

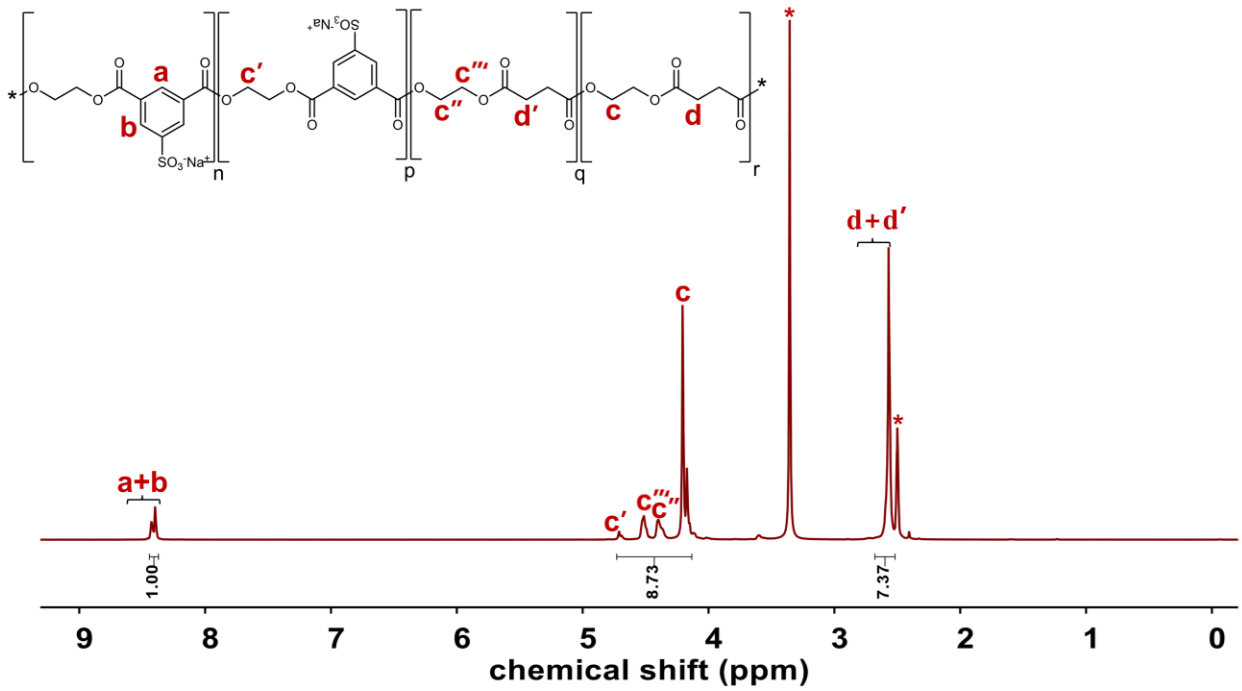

Figure S5. ^{1}H NMR spectrum of PESSIPA0.15.

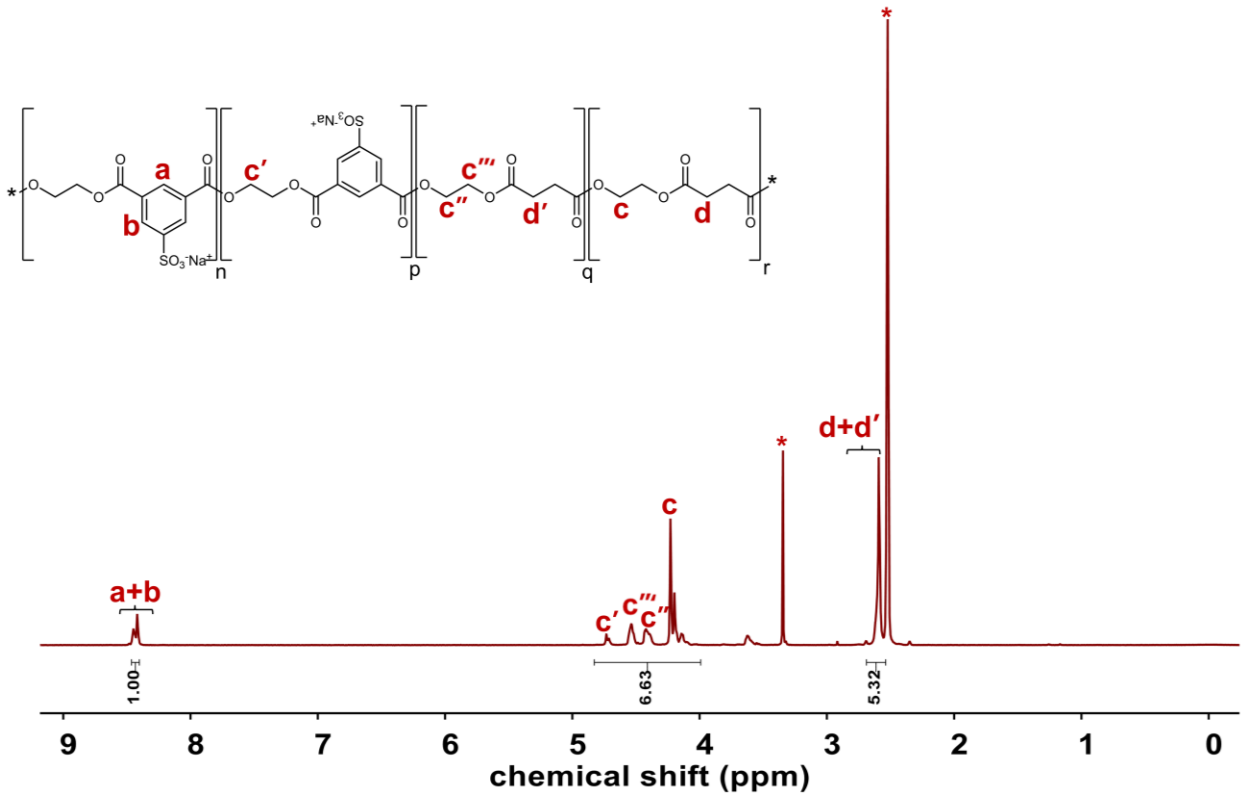

Figure S6. ^{1}H NMR spectrum of PESSIPA0.20.

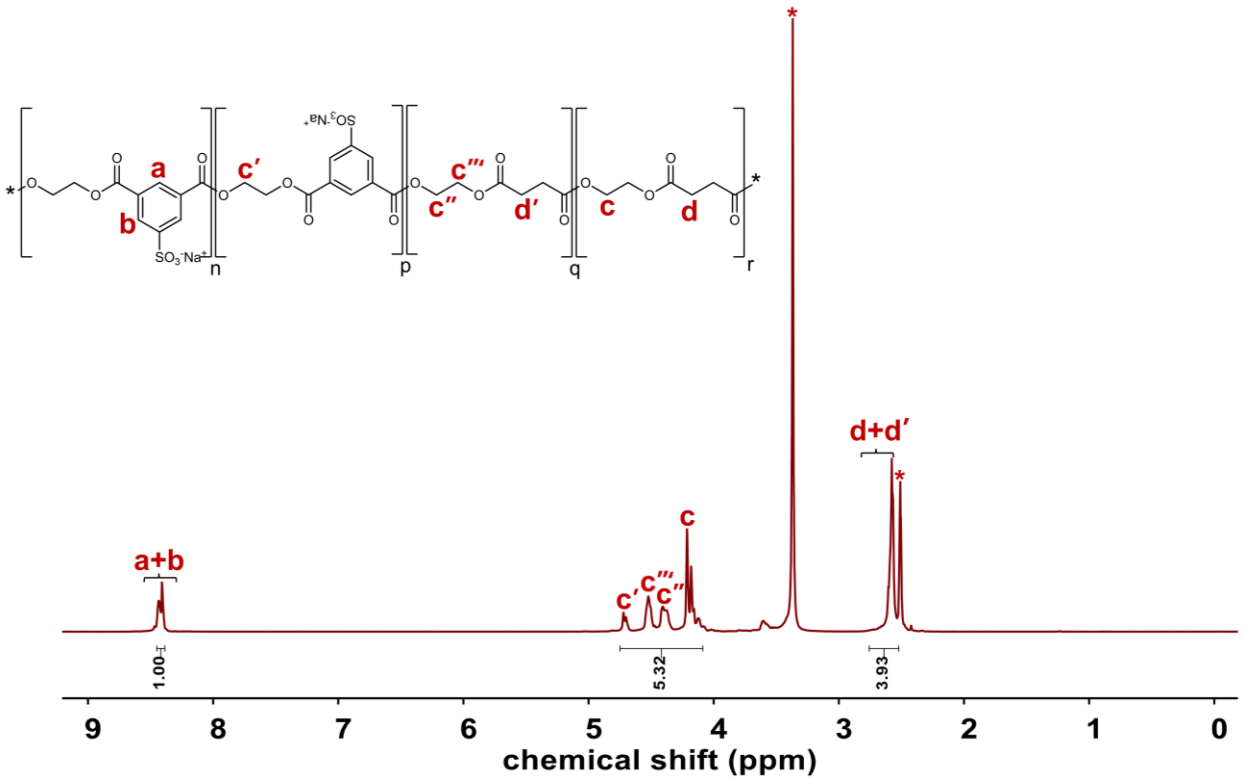

Figure S7. ^{1}H NMR spectrum of PESSIPA0.25.

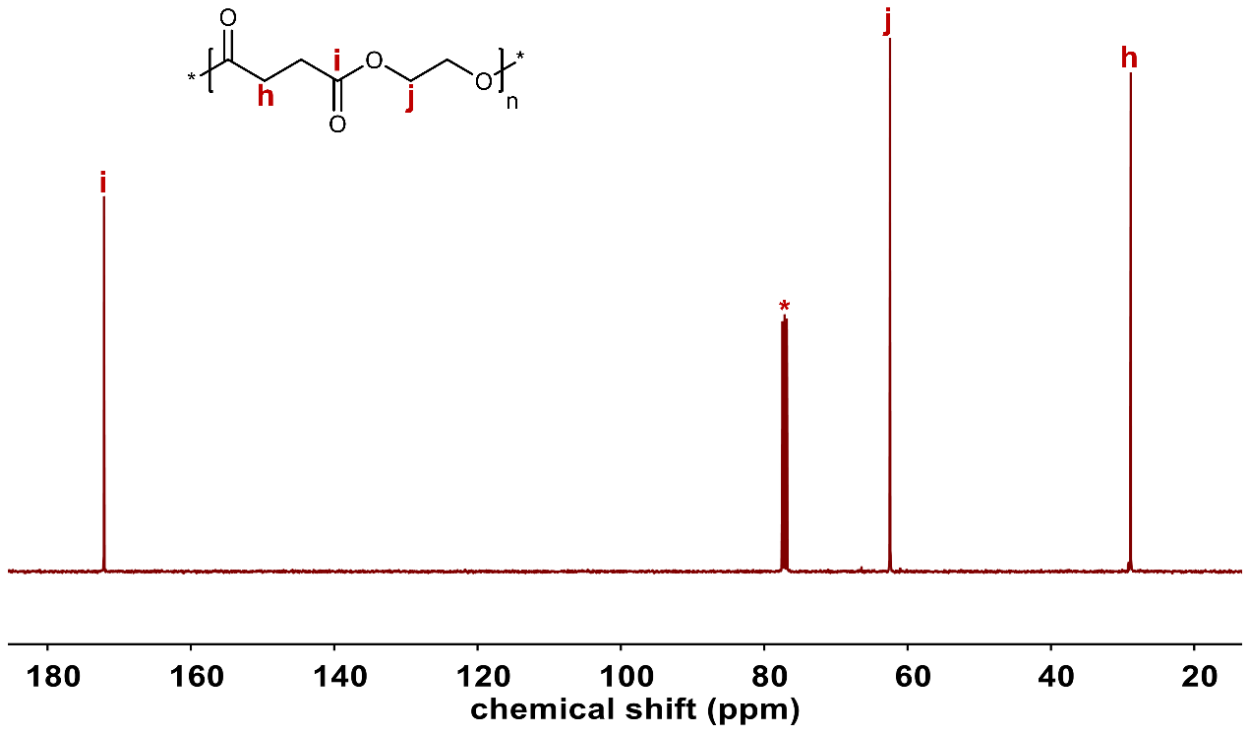

Figure S8. ^{13}C NMR spectrum of PES.

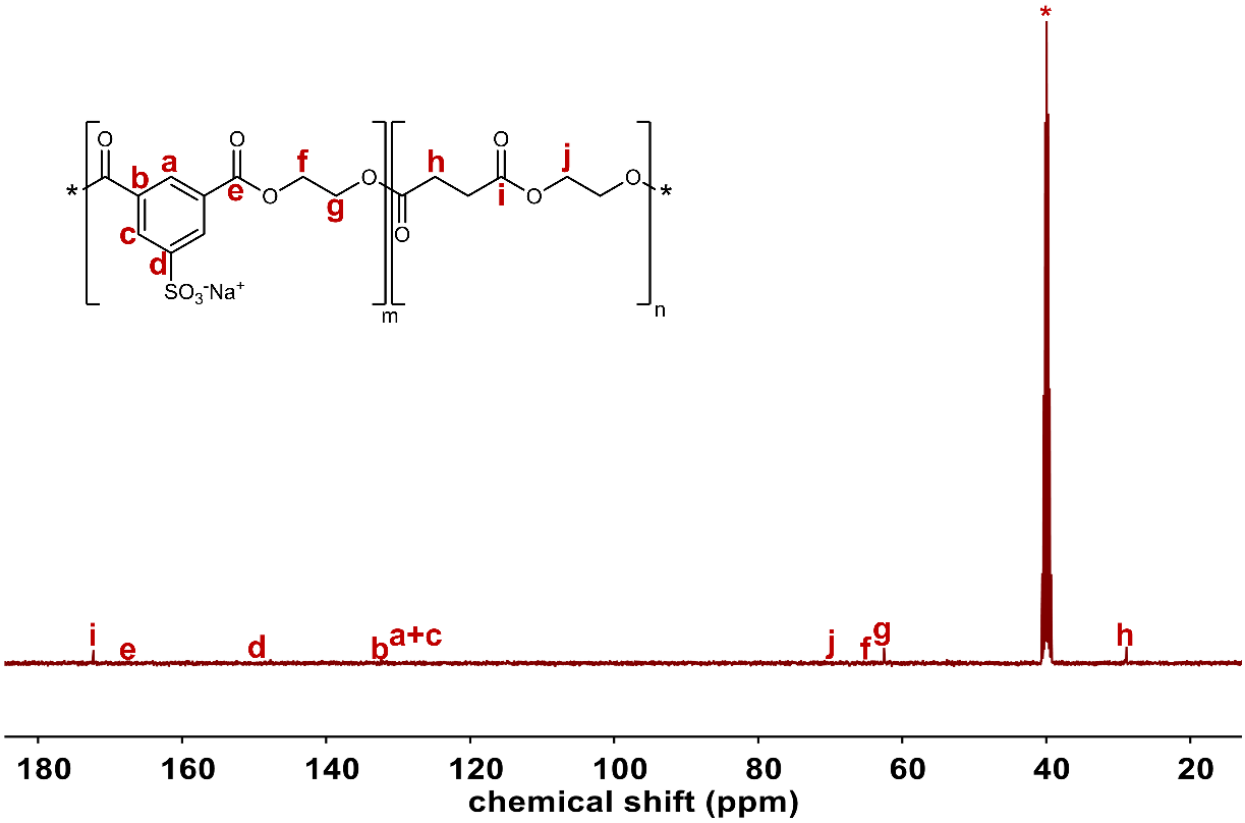

Figure S9. ^{13}C NMR spectrum of PESSIPA0.05.

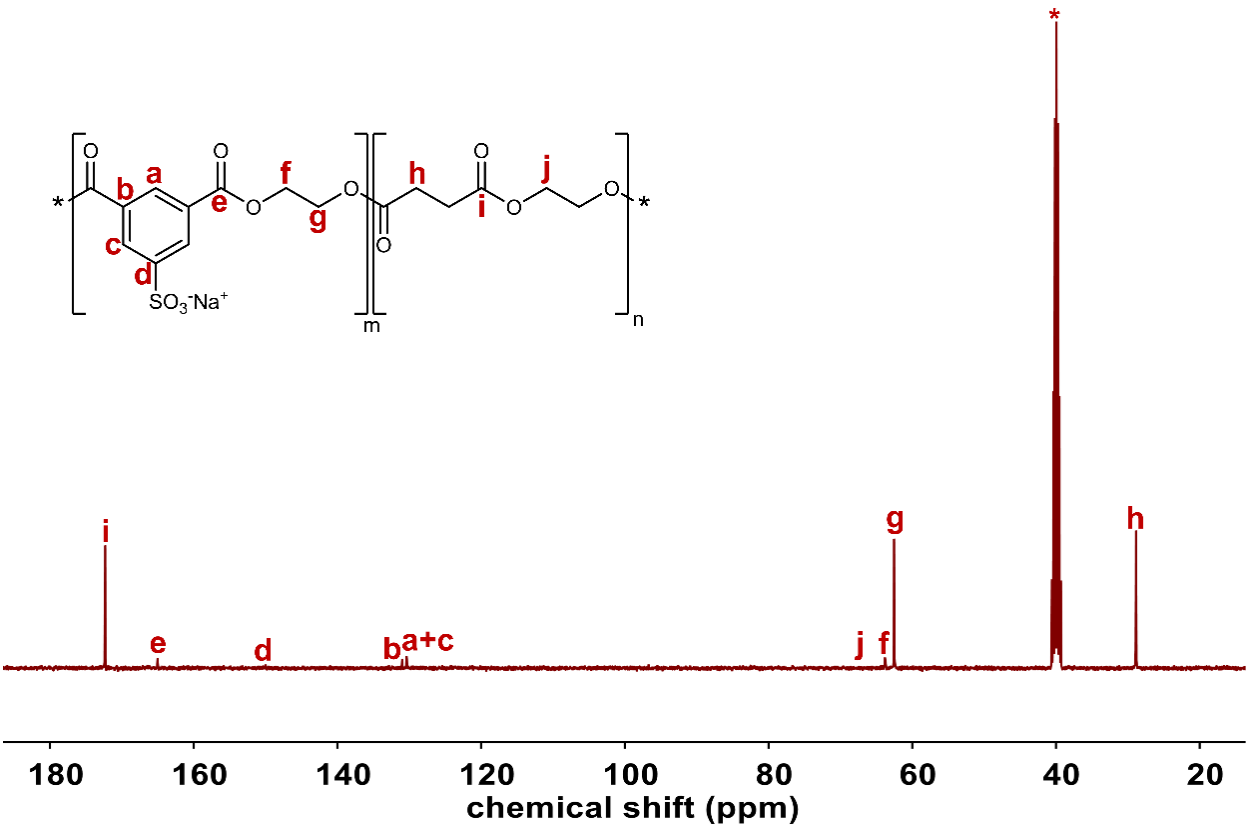

Figure S10. ^{13}C NMR spectrum of PESSIPA0.1.

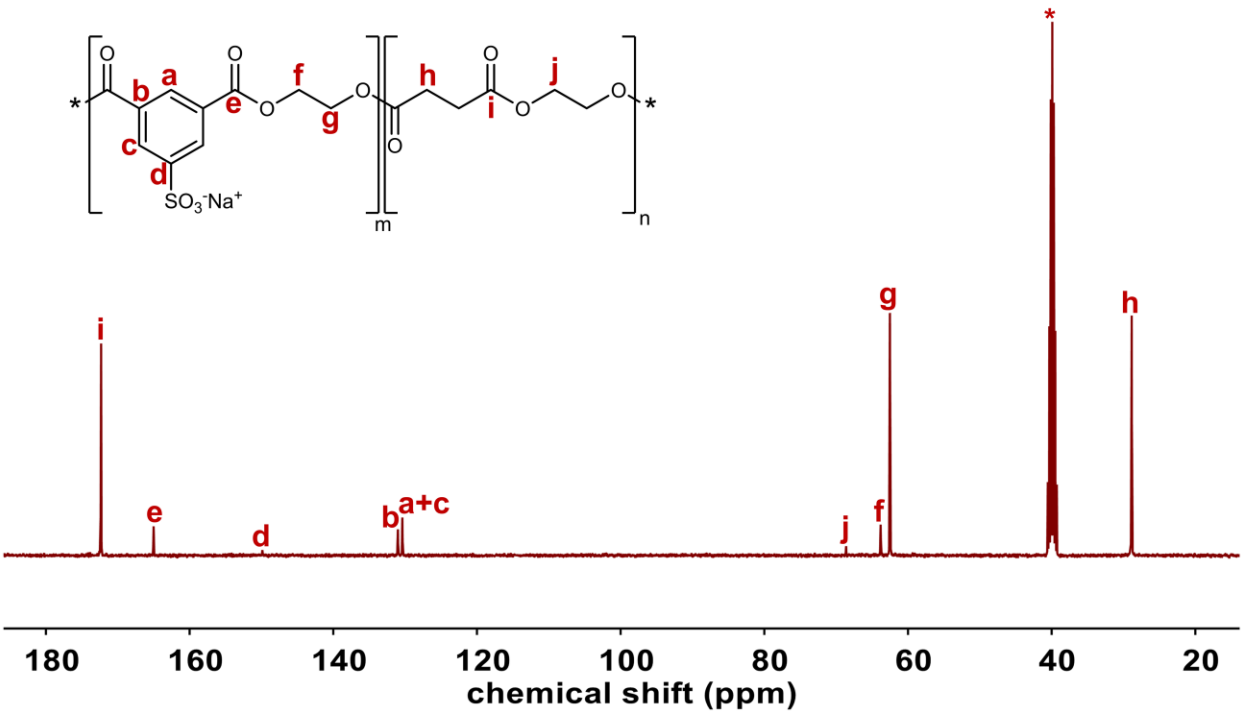

Figure S11. ^{13}C NMR spectrum of PESSIPA0.15.

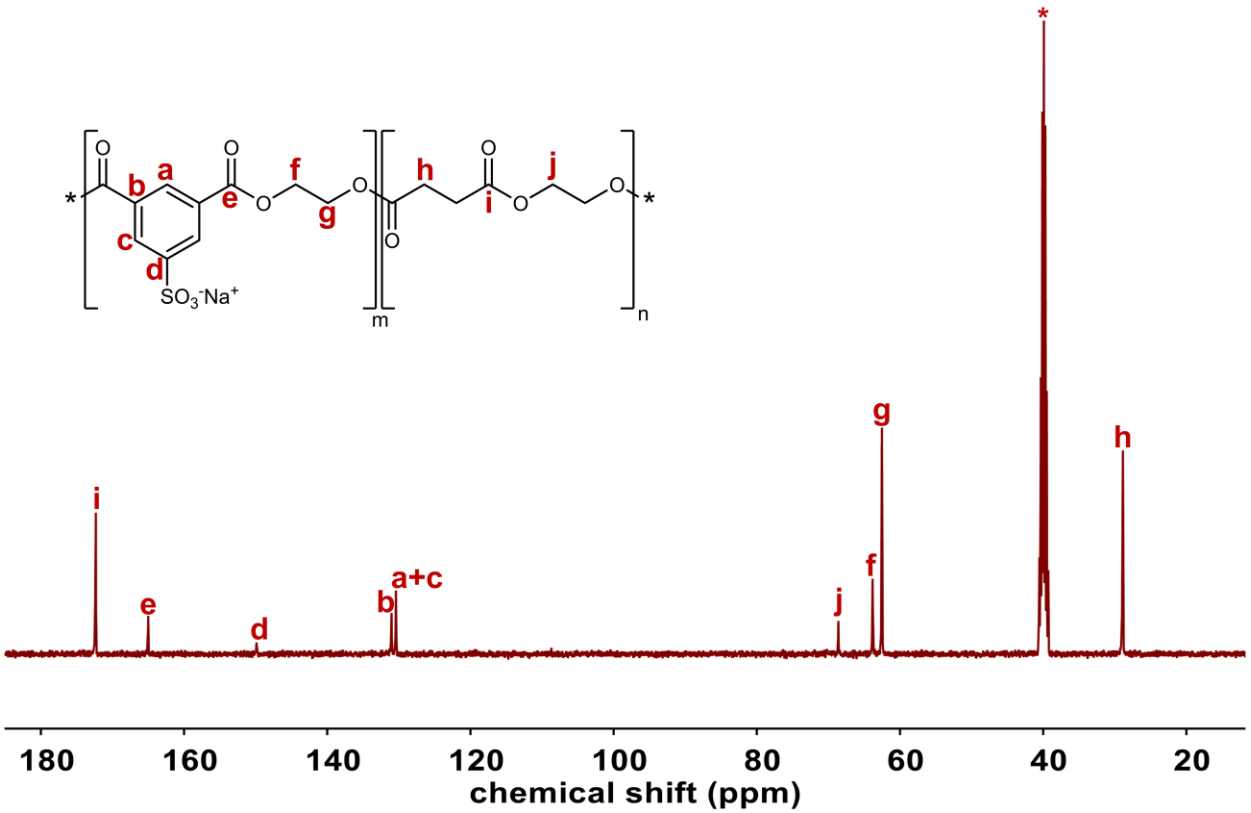

Figure S12. ^{13}C NMR spectrum of PESSIPA0.2.

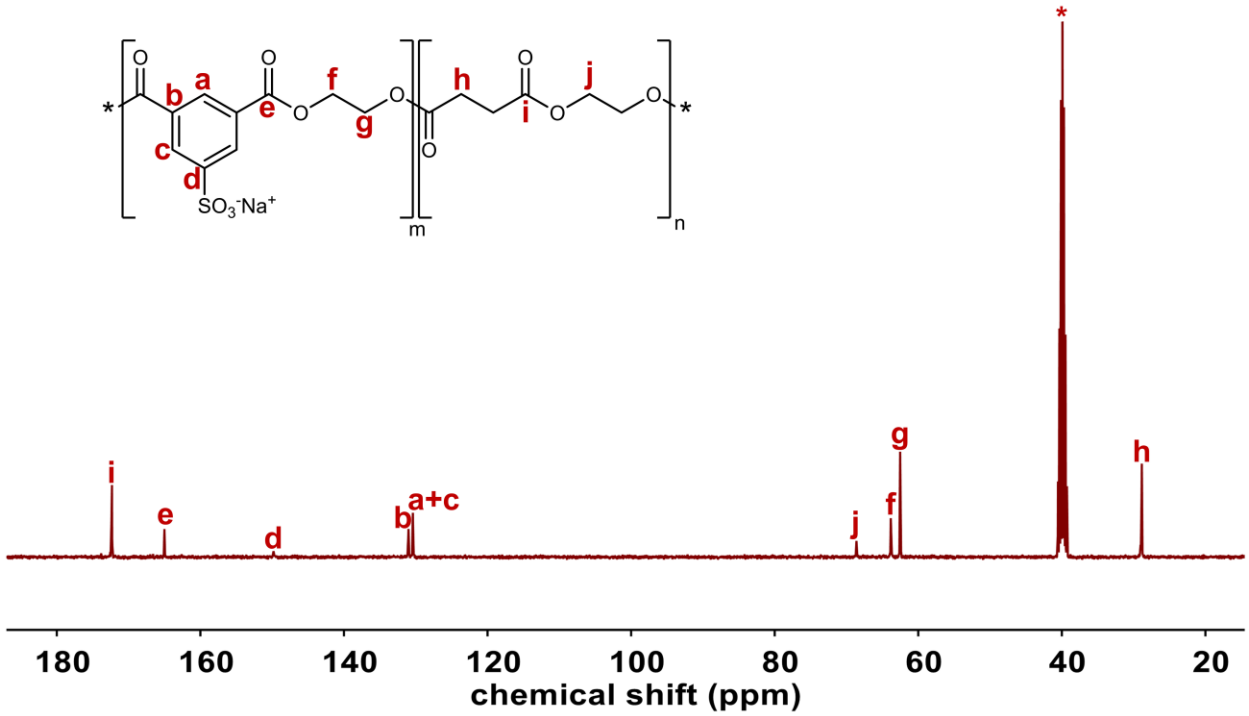

Figure S13. ^{13}C NMR spectrum of PESSIPA0.25.

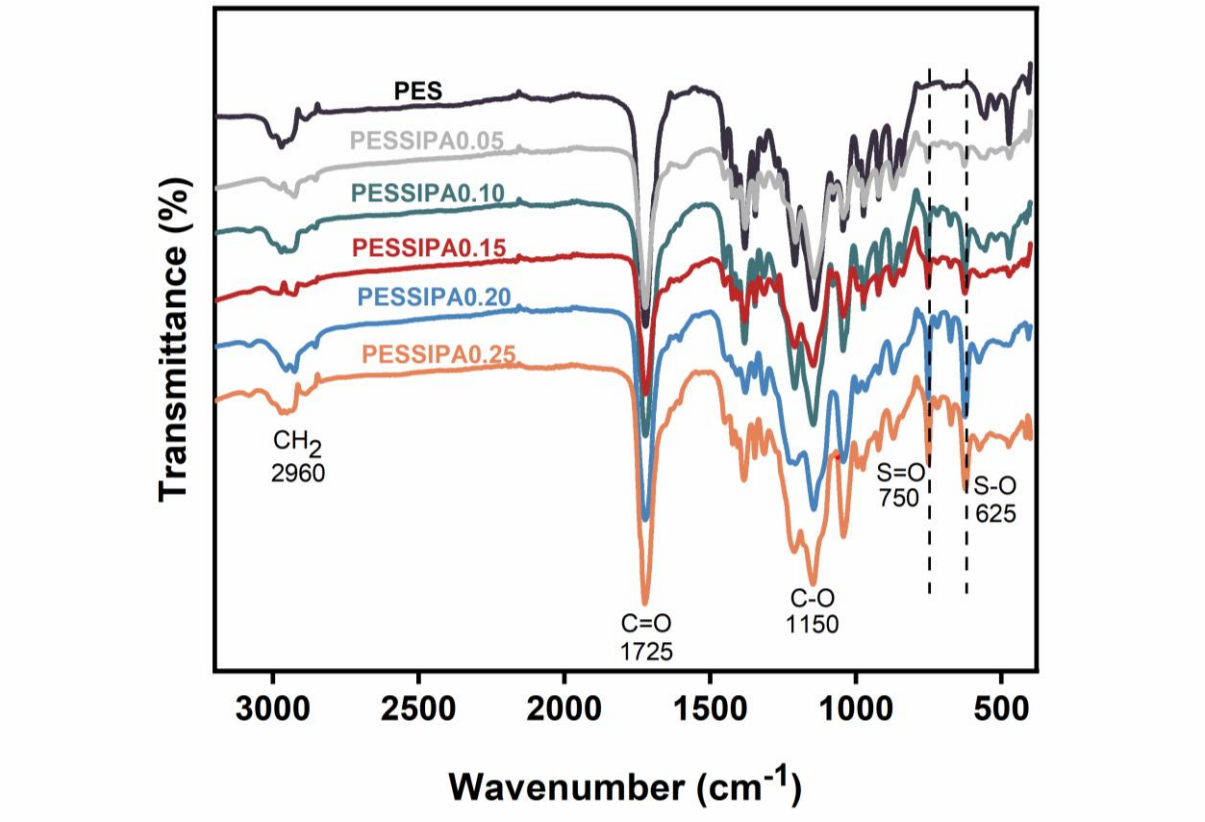

Figure S14. ATR-FTIR of products.

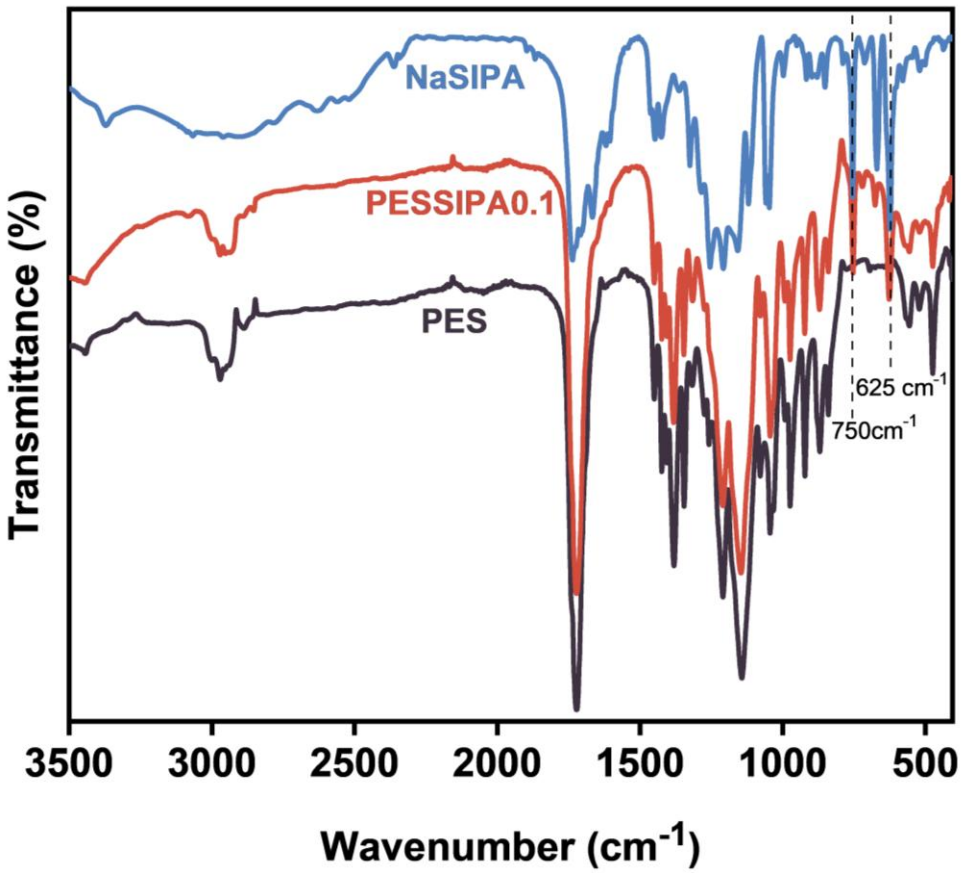

Figure S15. ATR-FTIR spectra of NaSIPA, PES, and PESSIPA0.1

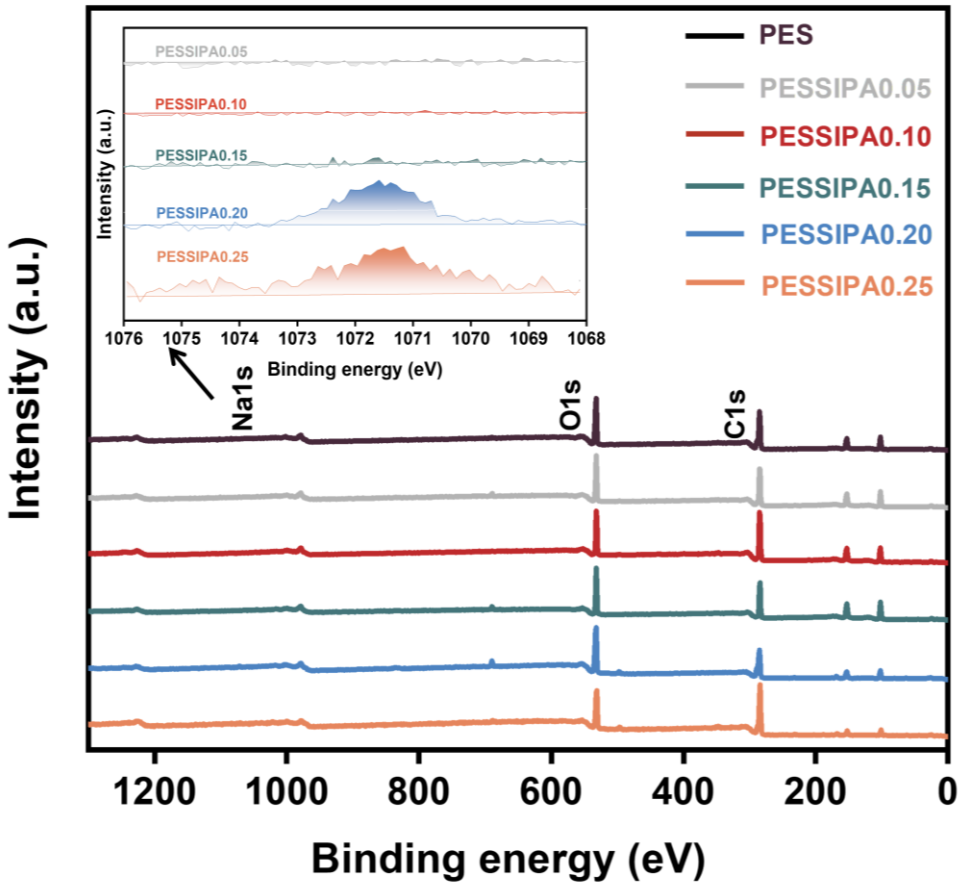

Figure S16. XPS of products.

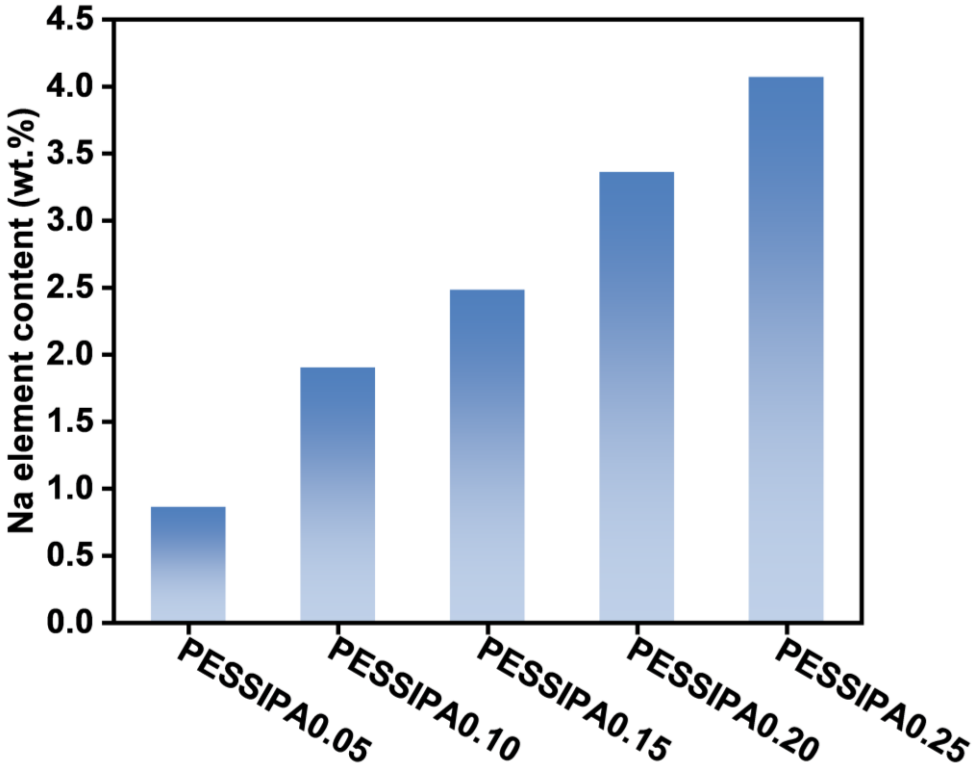

Figure S17. ICP-OES of PESSIPAs.

Figure S18. White sublimates formed during the polyesterification process.

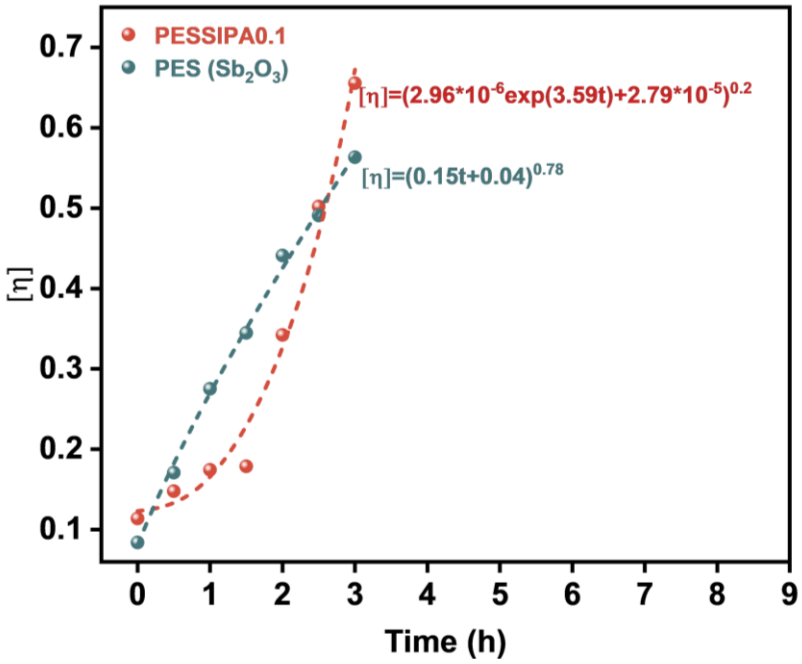

Figure S19. Comparison of polymerization kinetics between Catalyst-free PESSIPA0.1 and metal catalyst (Sb_2O_3)-catalyzed PES.

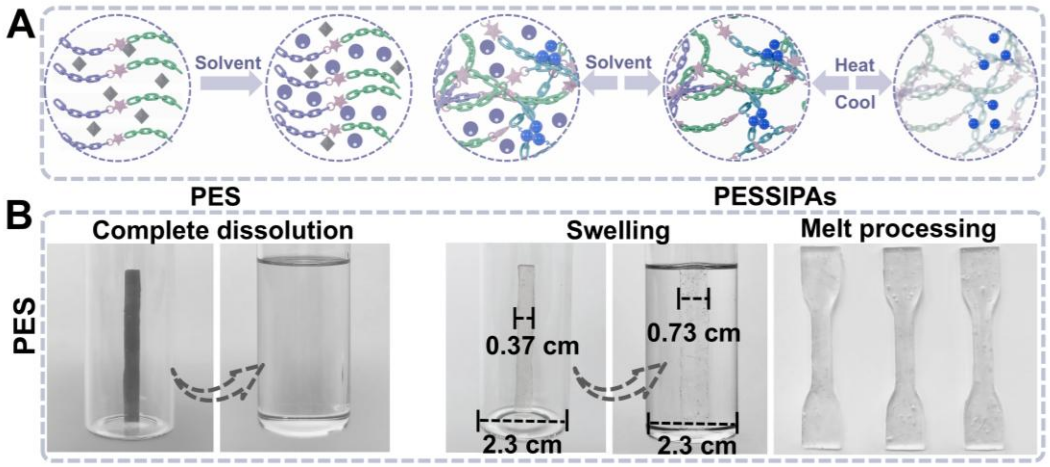

Figure S20. Aggregation characterization. A, Schematic diagram of dynamic cross-linking. **B,** Solubility in organic solvents, high-temperature melt processability.

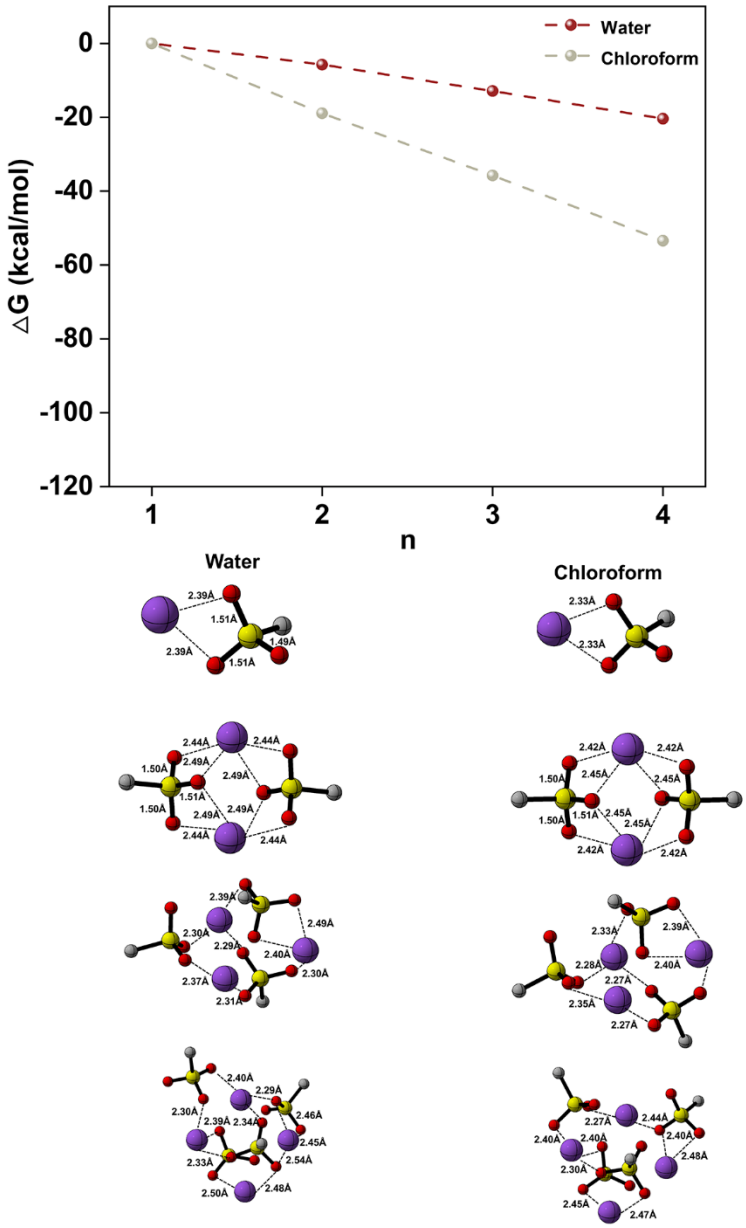

Figure S21. Calculation of energy differences in various aggregates using M06-2X/6-311++G(d, p) n-mer: n monomers aggregated. All the single-point energies obtained from the optimized structures were corrected using a frequency scale factor of 0.9700 via Shermo 2.6.

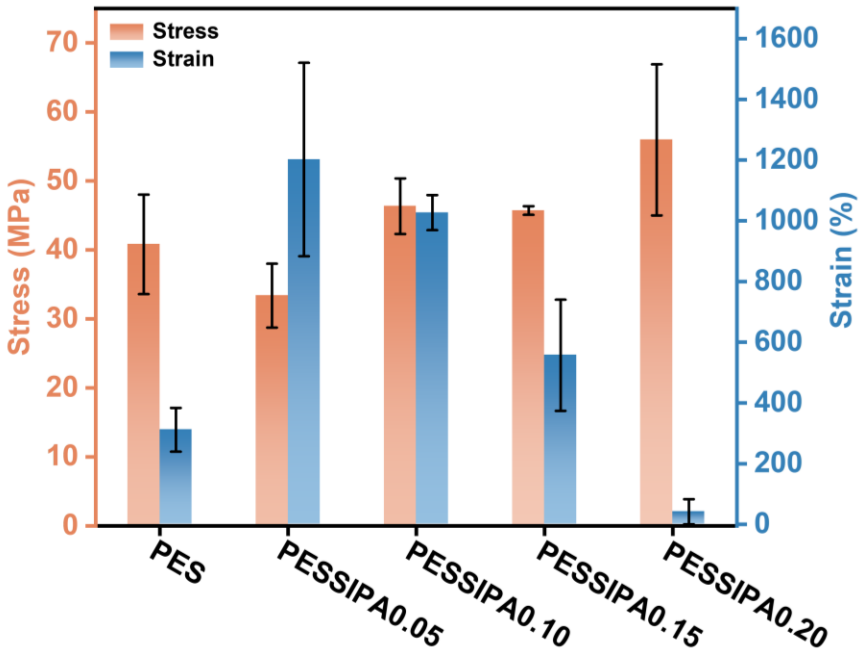

Figure S22. Tensile Properties of PES and PESSIPAs. Error bars represent standard deviation, n = 5.

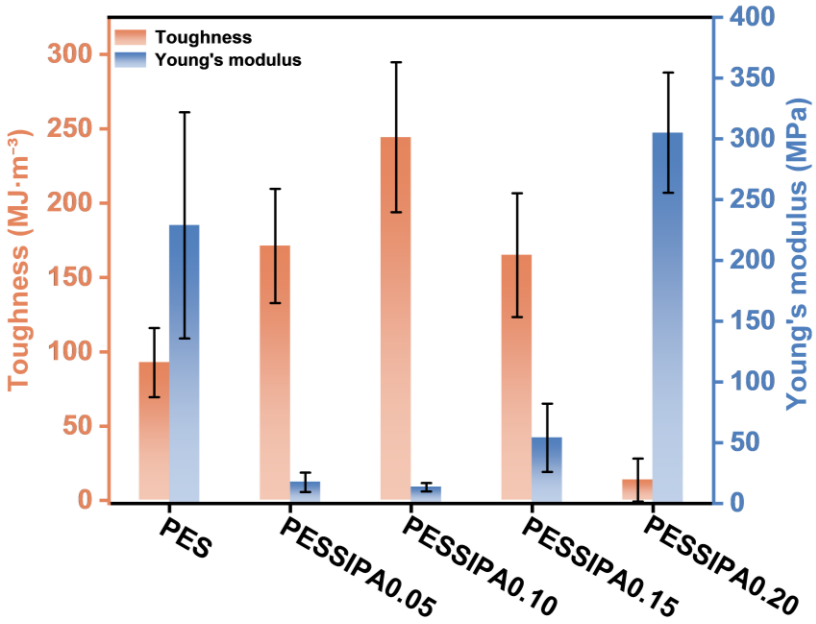

Figure S23. Tensile Properties of PES and PESSIPAs. Error bars represent standard deviation, n = 5.

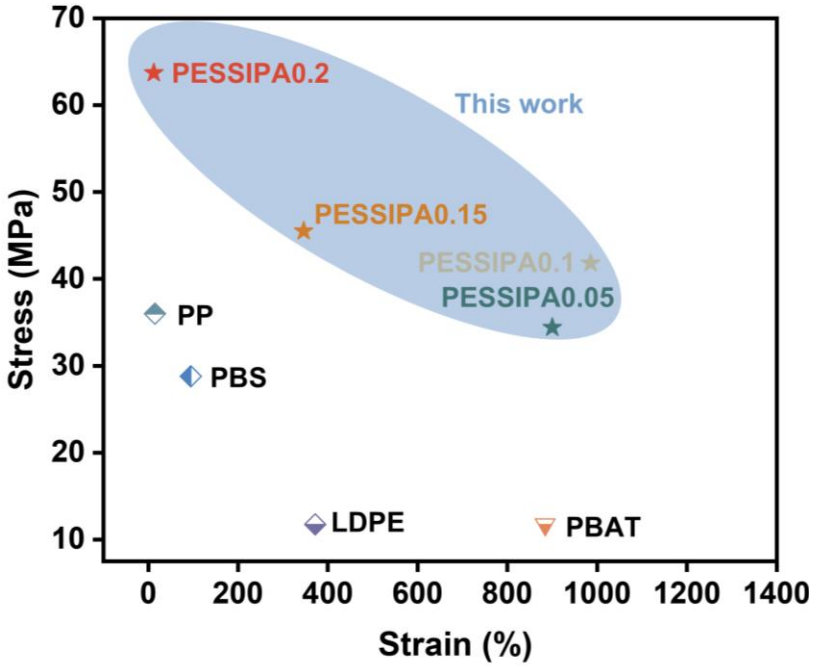

Figure S24.Comparison of mechanical properties between PESSIPAs and several commercial polymers. PP, polypropylene; LDPE, low density polyethylene; PBS, poly(butylene succinate); Poly(butylene adipate-co-terephthalate).

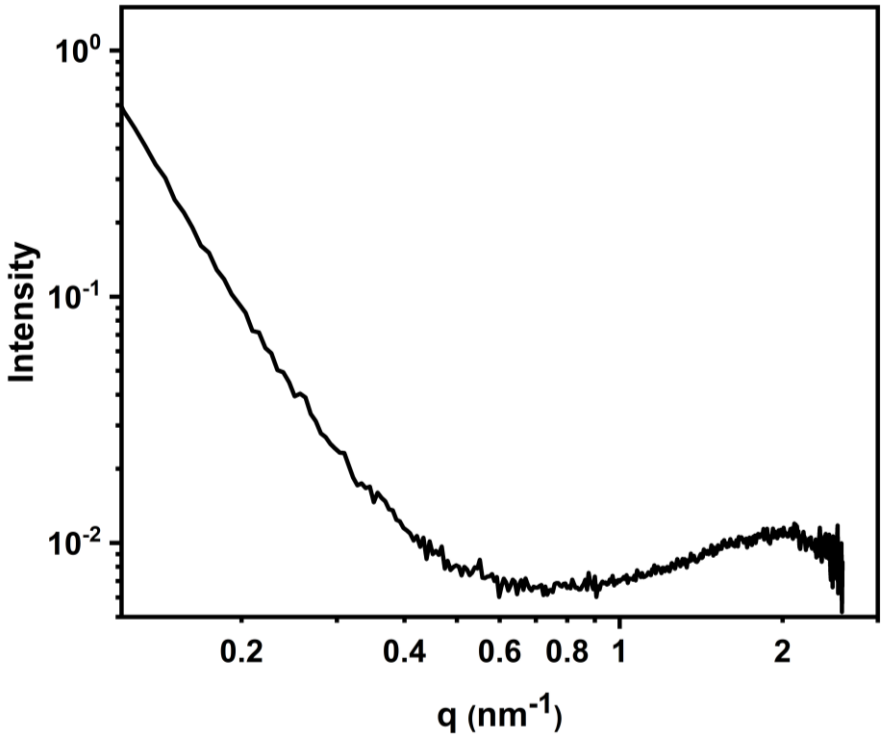

Figure S25. SAXS one-dimensional curve of PESSIPA0.1 at 300% strain state.

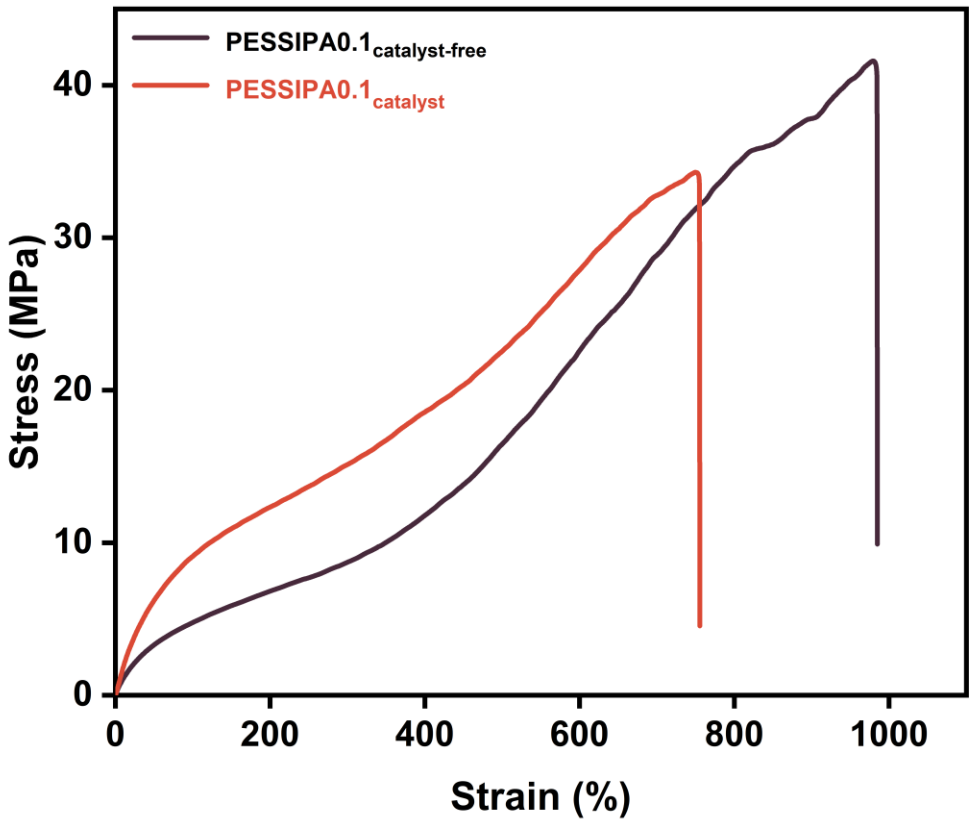

Figure S26. Tensile properties of PESSIPA0.1 with (PESSIPA0.1$_{\text{catalyst-free}}$) or without catalyst (PESSIPA0.1$_{\text{catalyst}}$).

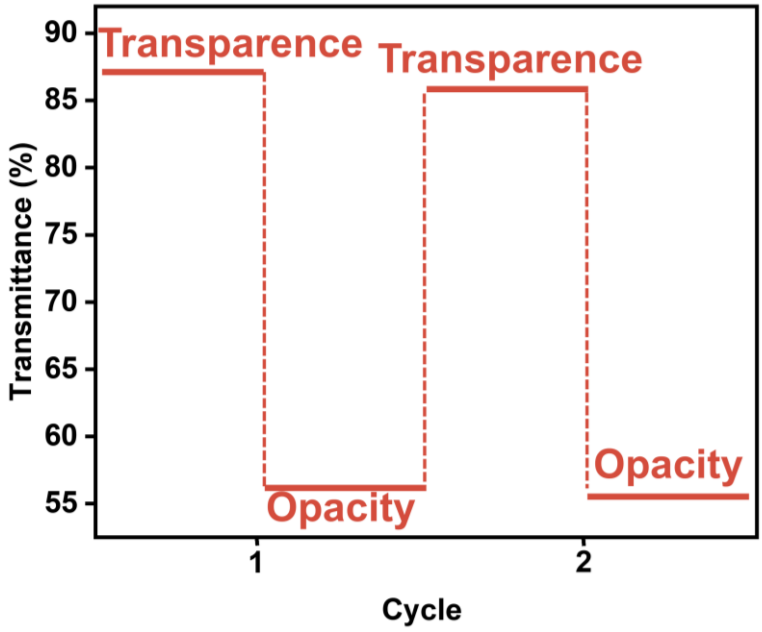

Figure S27. Change in transmittance of PESSIPA0.1 between transparent and opaque states.

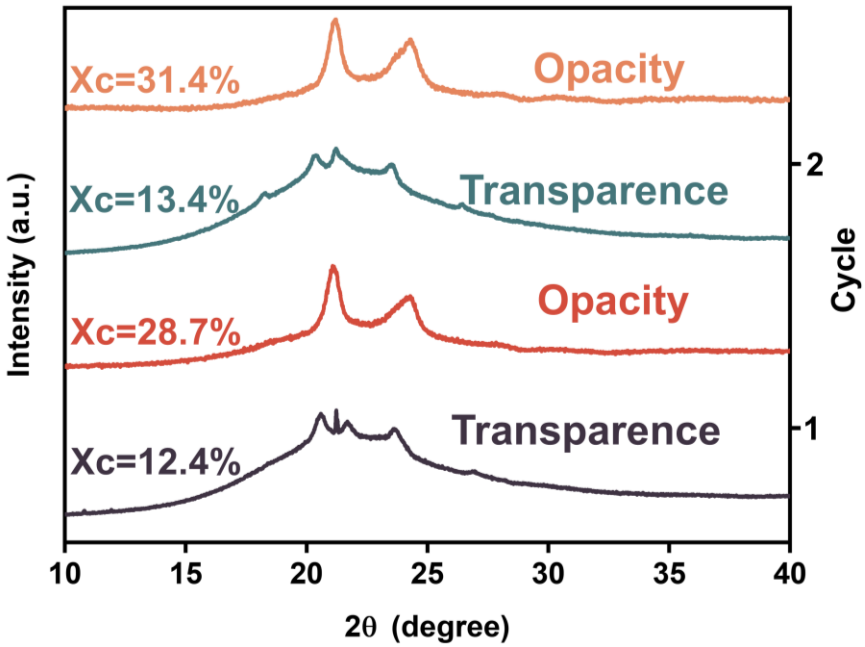

Figure S28. Change in crystallinity of PESSIPA0.1 between transparent and opaque states.

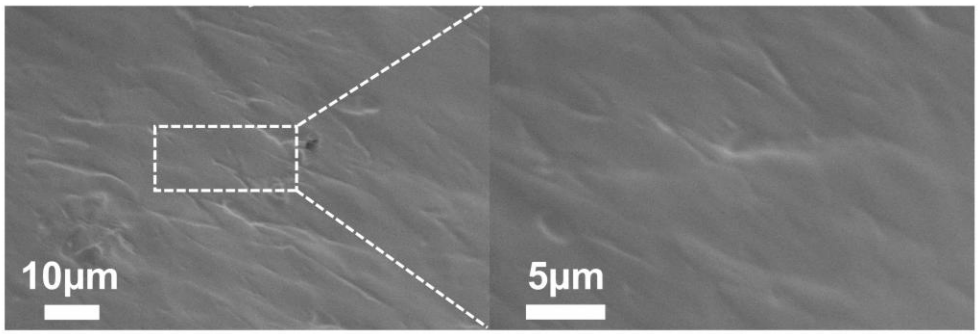

Figure S29. SEM images of unwelded section of PESSIPA0.1.

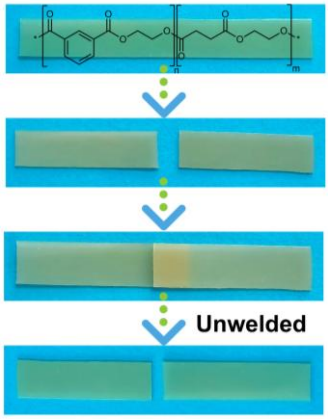

Figure S30. Schematic diagram of the welding performance test for PESIPA0.1.

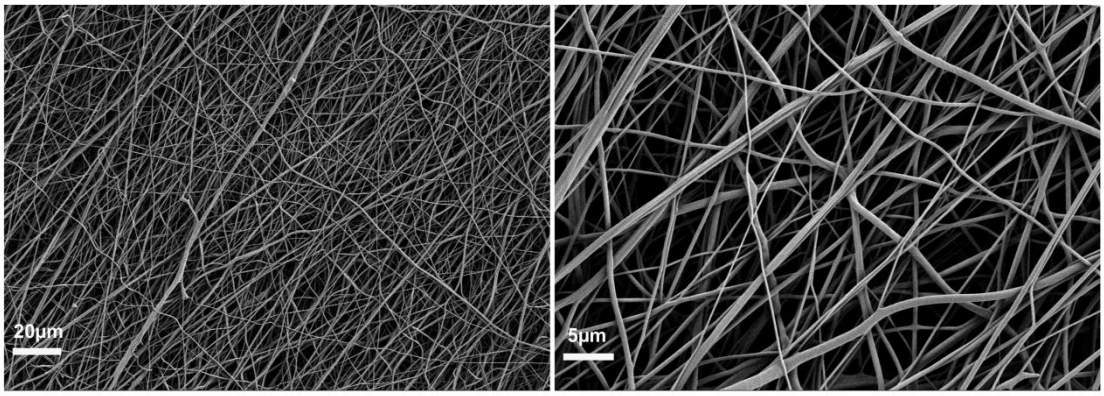

Figure S31. SEM images of PESSIPA0.1 after electrospinning.

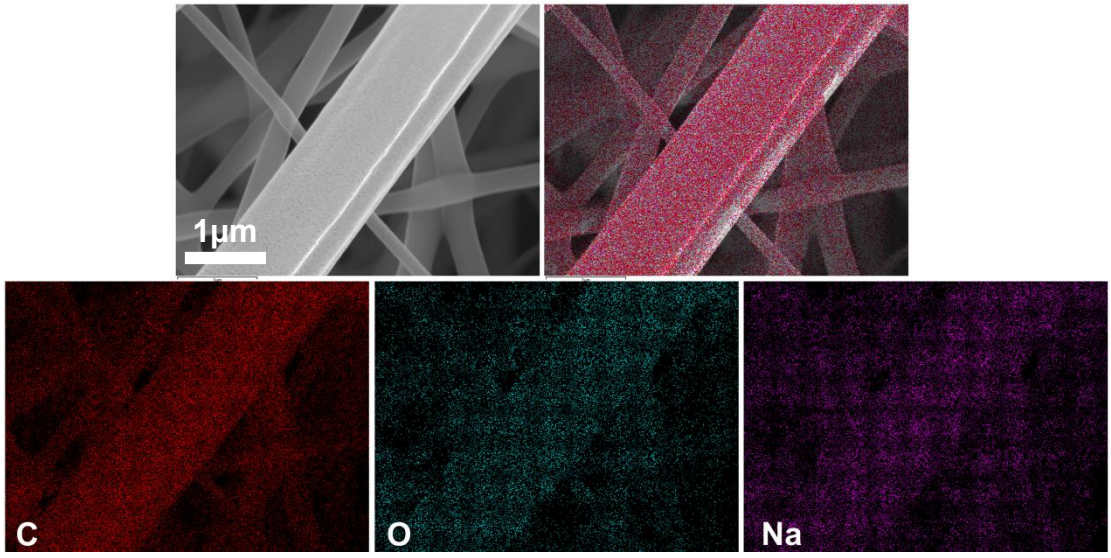

Figure S32. EDS energy spectrum of PESSIPA0.1 fiber.

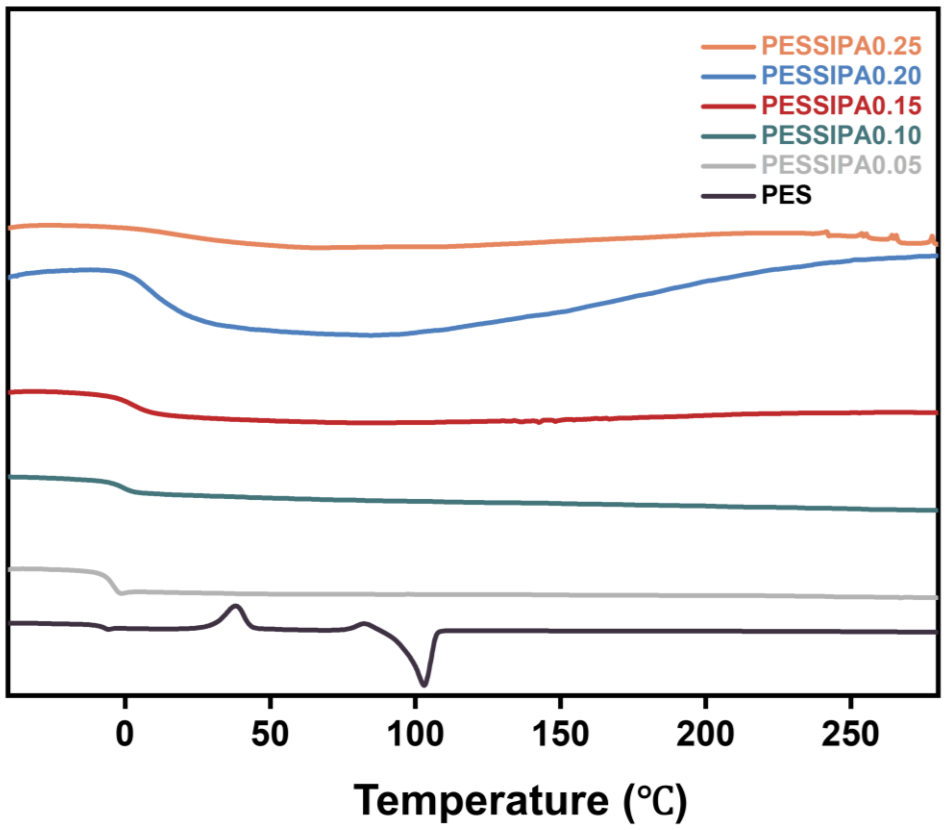

Figure S33. DSC of products.

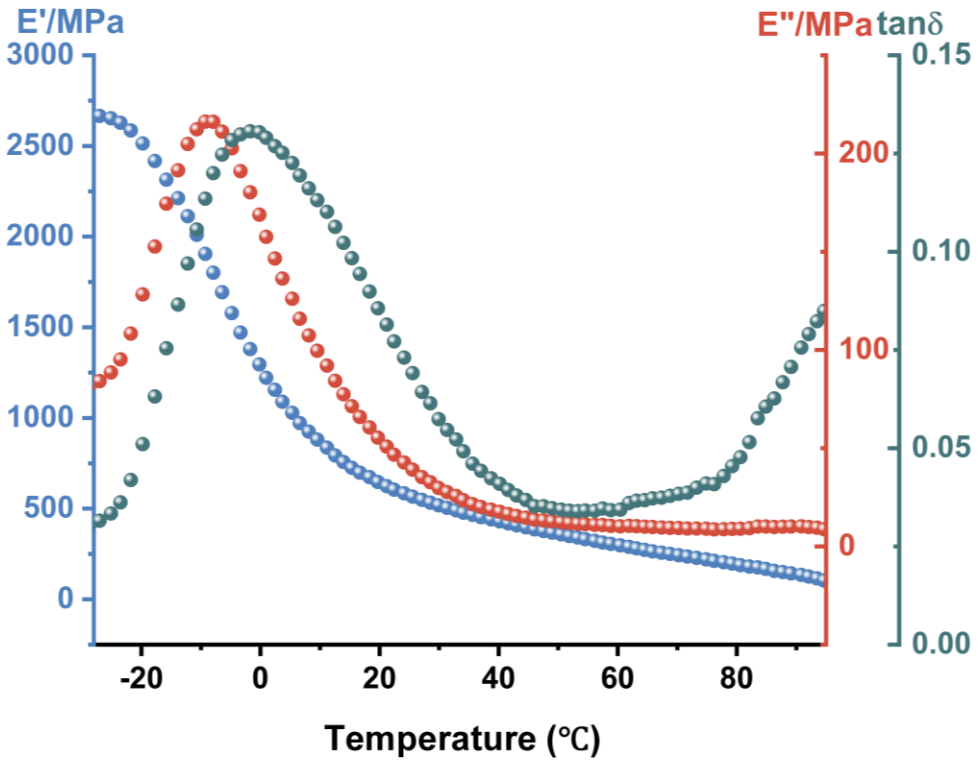

Figure S34. Loss factor (tan δ), storage modulus (E'), and loss modulus (E'') of the PES.

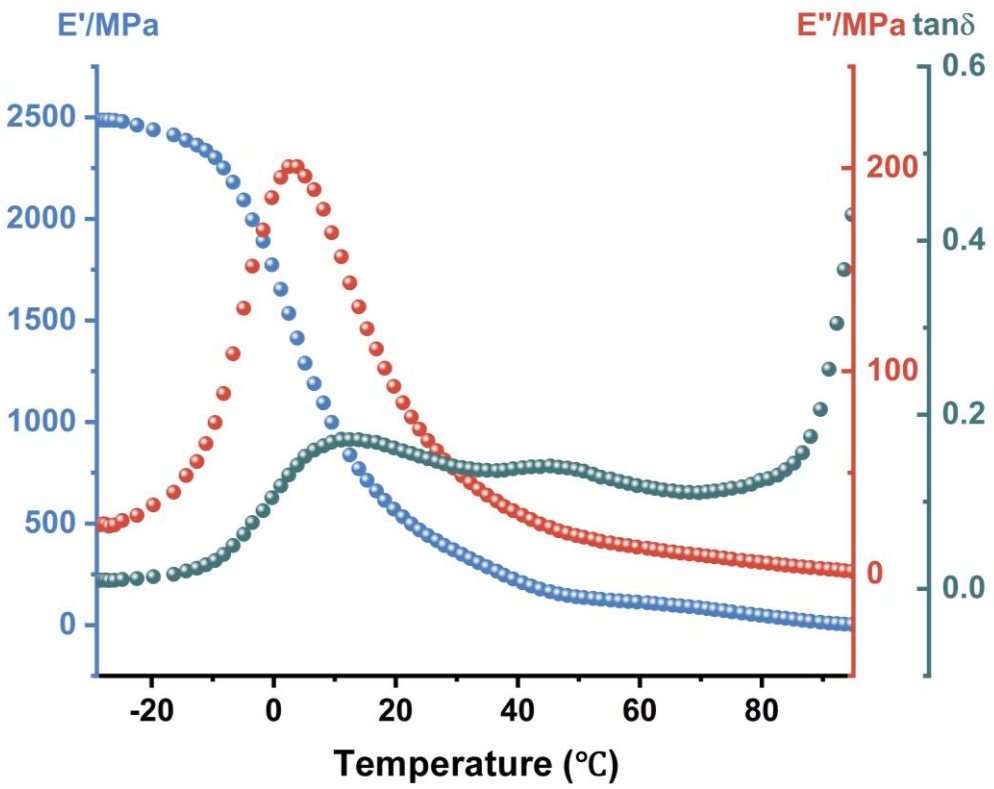

Figure S35. Loss factor (tan δ), storage modulus (E'), and loss modulus (E'') of the PESSIPA0.05.

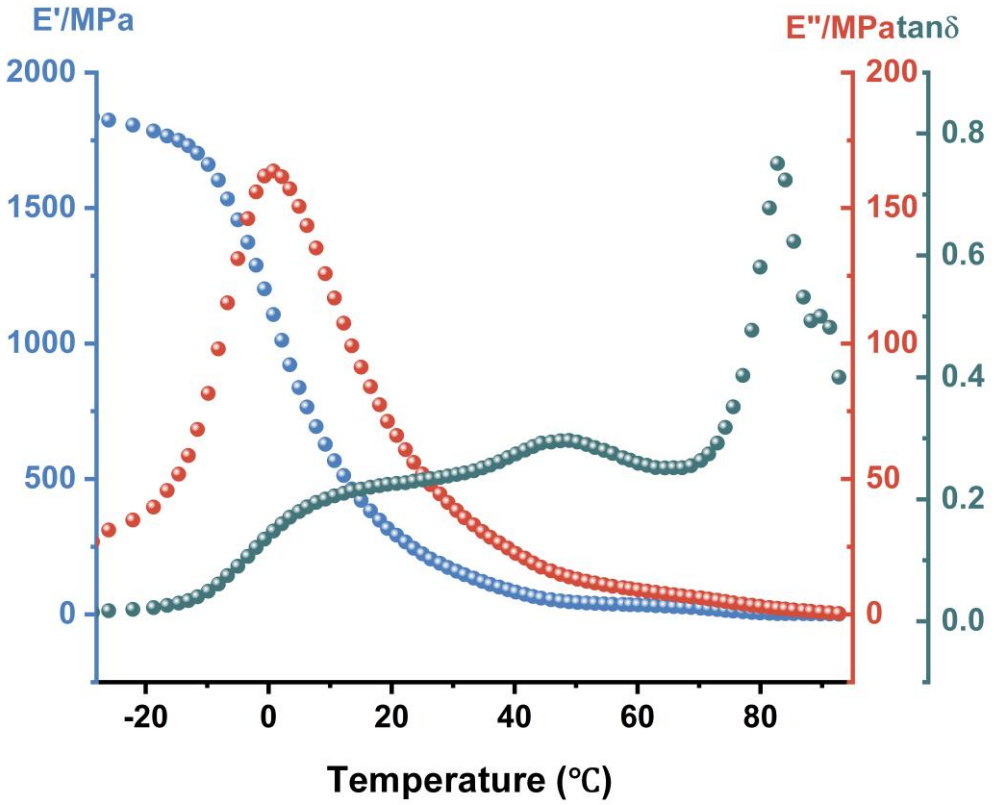

Figure S36. Loss factor (tan δ), storage modulus (E'), and loss modulus (E'') of the PESSIPA0.10.

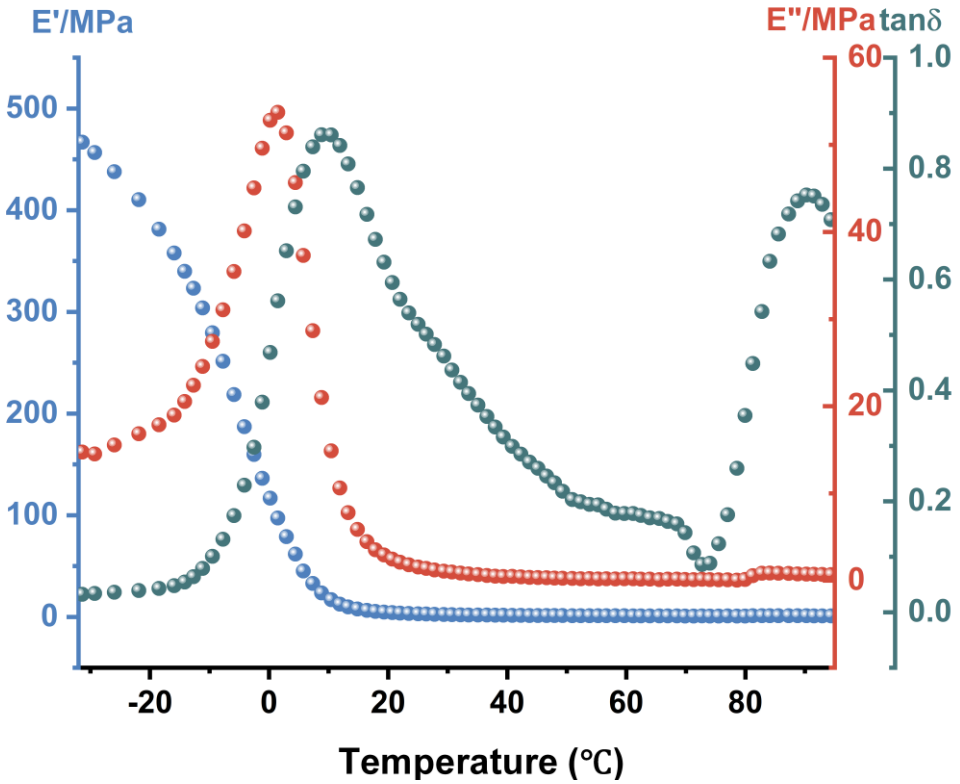

Figure S37. Loss factor (tan δ), storage modulus (E'), and loss modulus (E'') of the PESSIPA0.15.

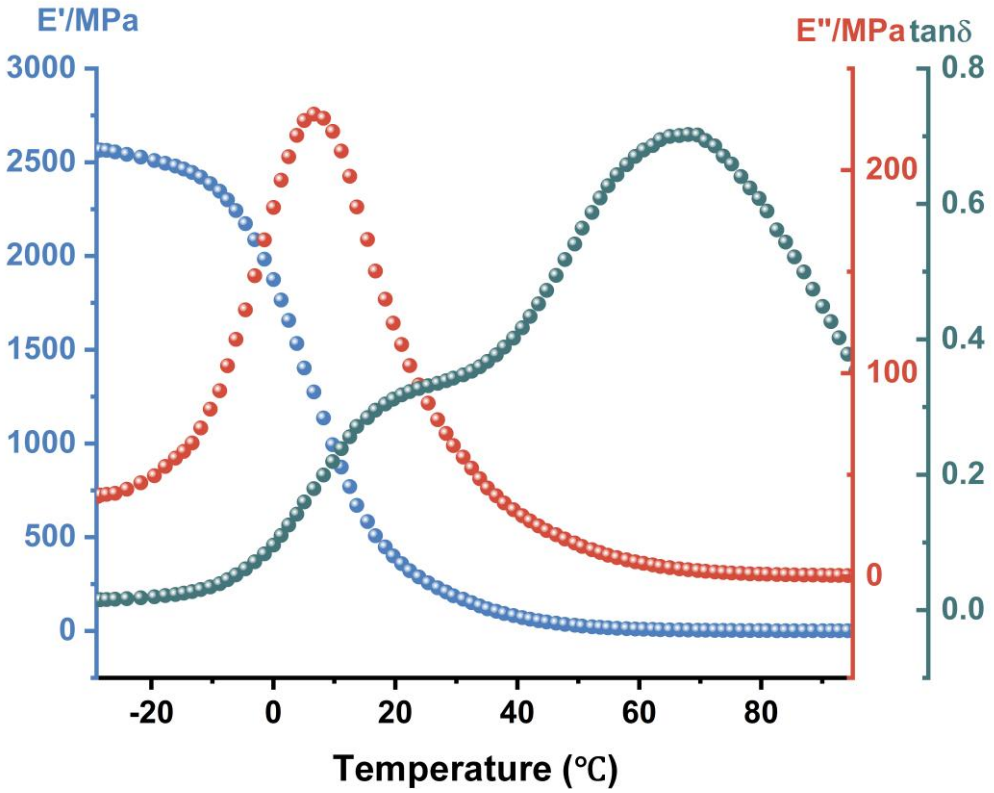

Figure S38. Loss factor (tan δ), storage modulus (E'), and loss modulus (E'') of the PESSIPA0.20.

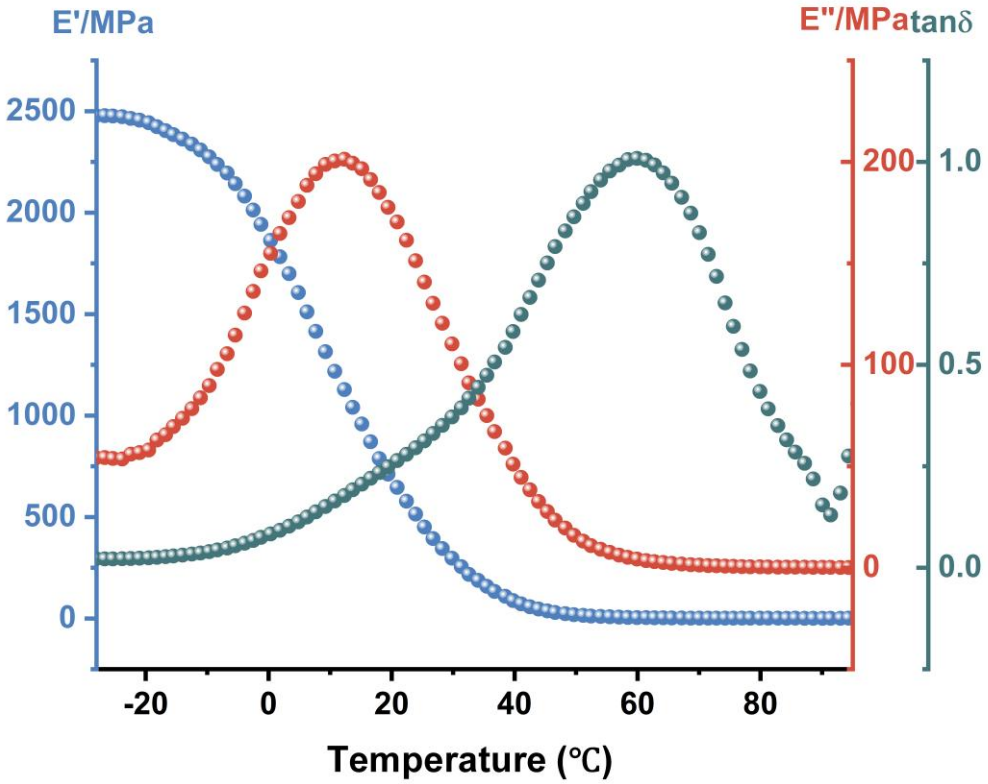

Figure S39. Loss factor (tan δ), storage modulus (E'), and loss modulus (E'') of the PESSIPA0.25.

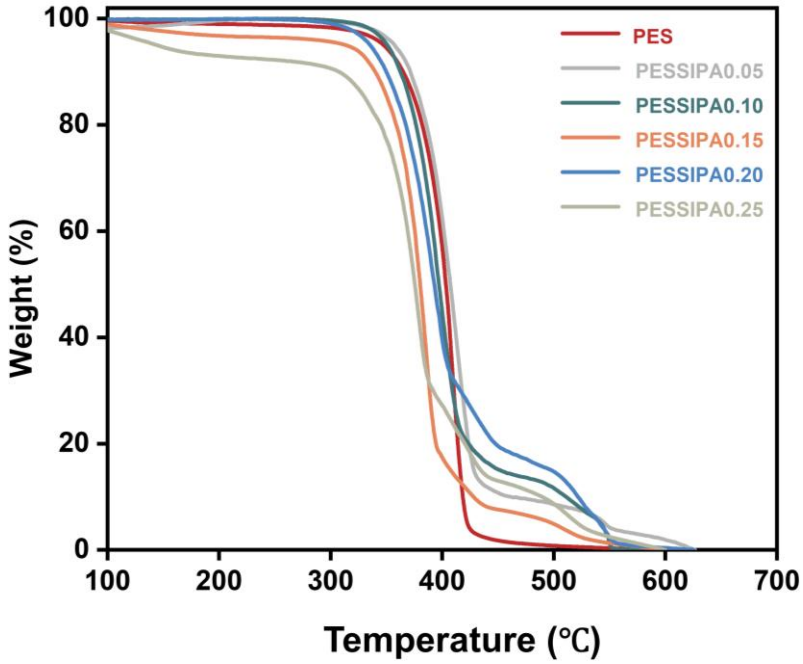

Figure S40. TGA of products.

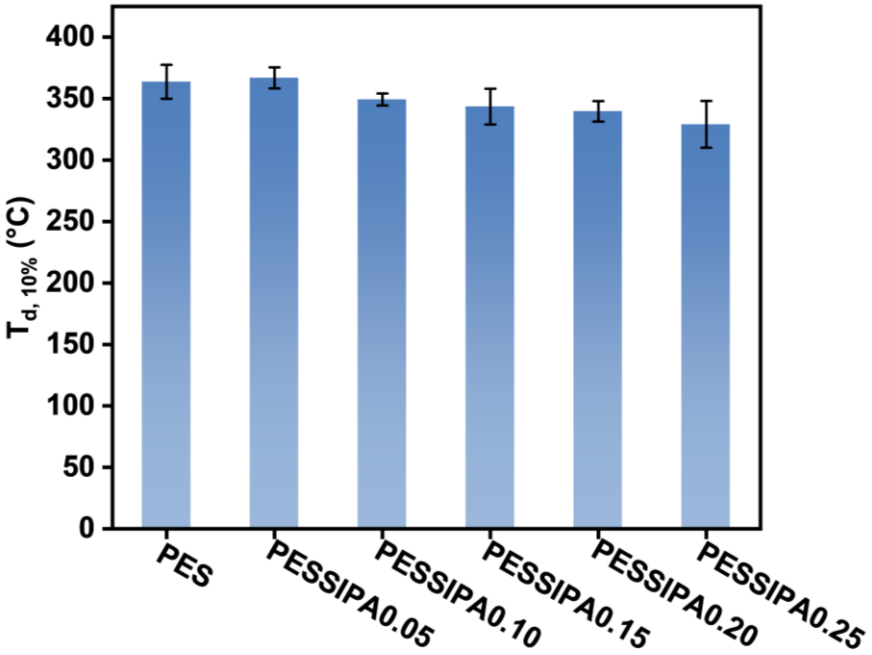

Figure S41. Decomposition temperatures of PES and PESSIPAs measured by TGA. Error bars represent standard deviation, n = 5.

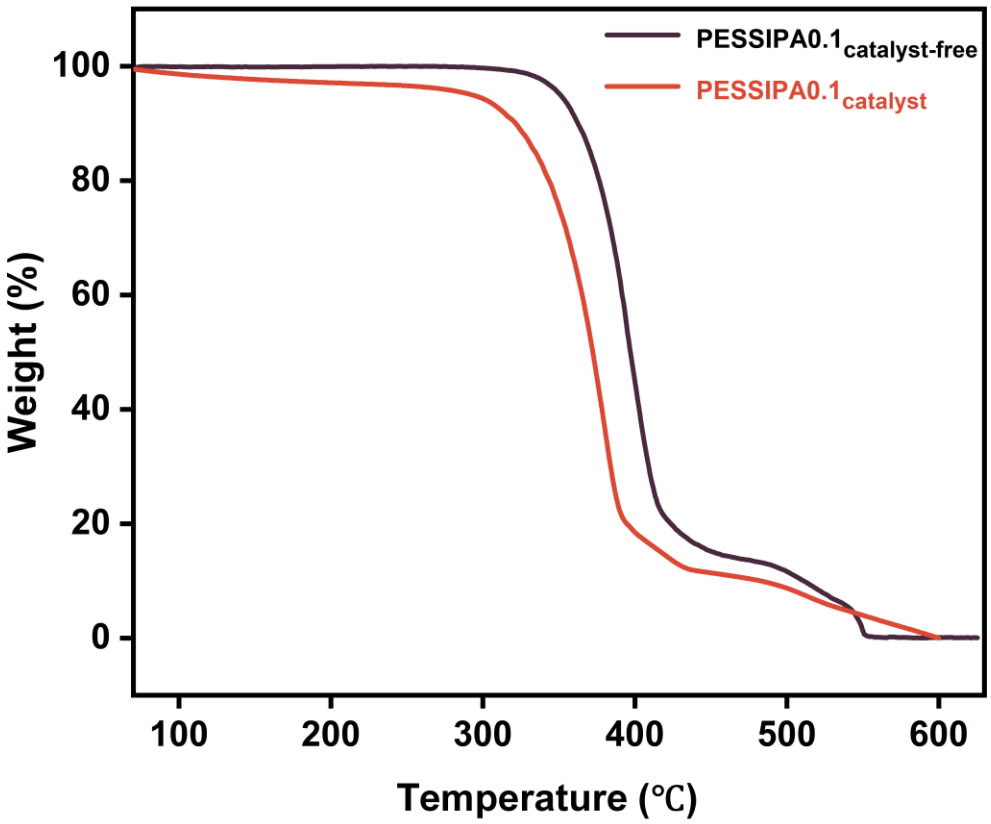

Figure S42. TGA of PESSIPA0.1 in the absence (PESSIPA0.1$_{\text{catalyst-free}}$) and presence (PESSIPA0.1$_{\text{catalyst}}$) of Sb_2O_3 catalyst.

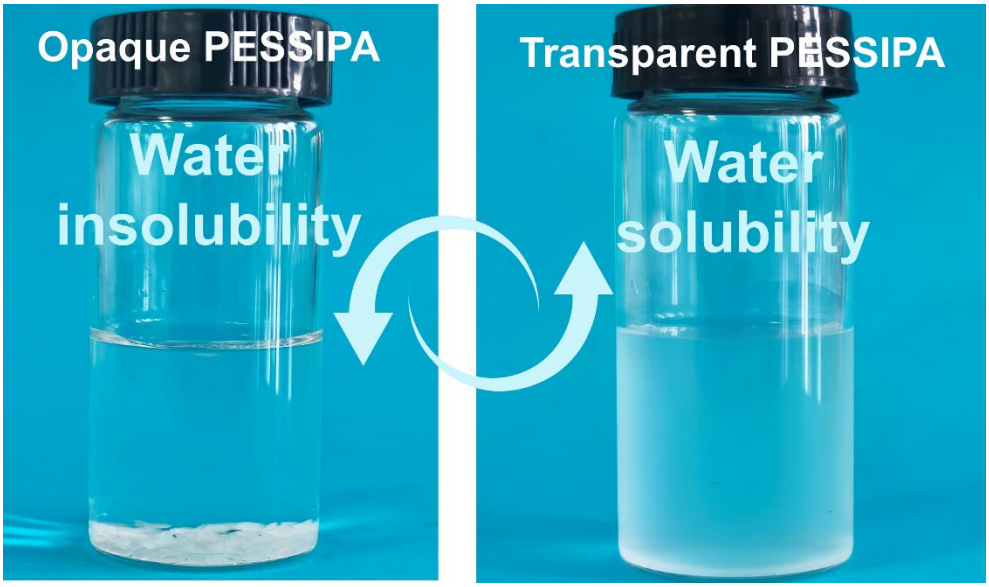

Figure S43. The water-soluble and insoluble switchable properties of PESSIPA0.1

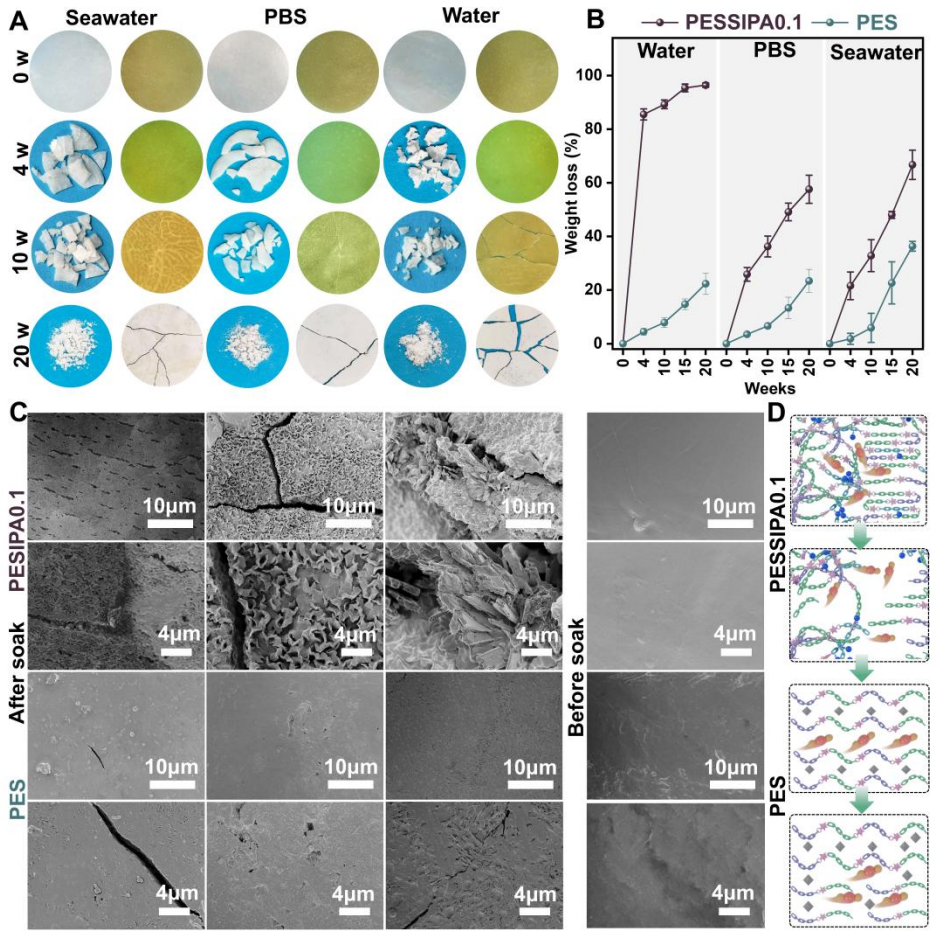

Figure S44. Degradation performance of PESSIPA0.1. A, Photographs of degradation under different conditions. **B**, Weight loss of PES and PESSIPA0.1. **C**, SEM images of PES and PESSIPA0.1 before and after immersion in various conditions for 10 weeks. Top: Scale bar = 10 μm; Down: Scale bar = 4 μm. **D**, Schematic diagram of degradation mechanism of PESSIPA0.1 and PES.

Figure S45. Approach to recycle PESSIPA0.1 from mixed plastics. Solvent: water.

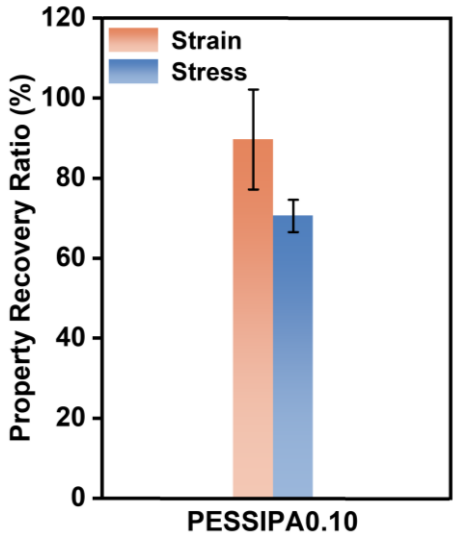

Figure S46. Mechanical property retention rate of the recycled PES-SIPA0.1 material, n = 3.

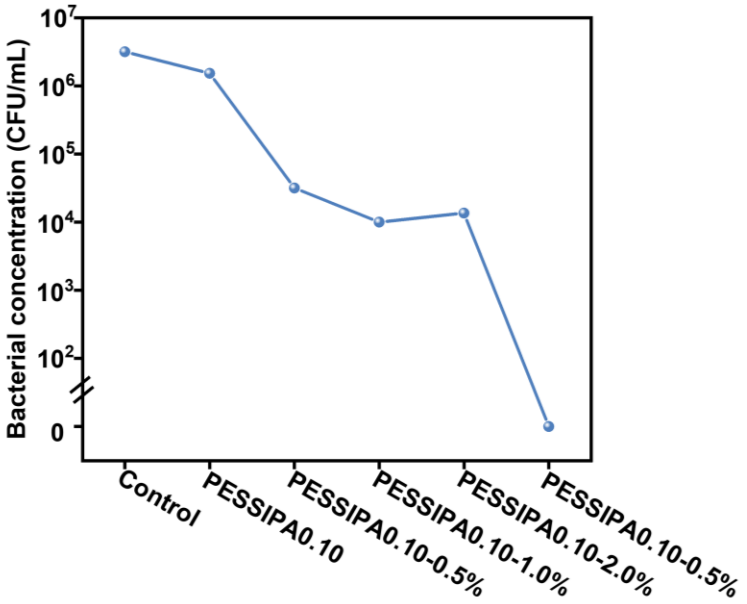

Figure S47. Antibacterial activity using E.coli. Molar fraction: 0.5-4.0%. Error bars represent standard deviation, n = 3.

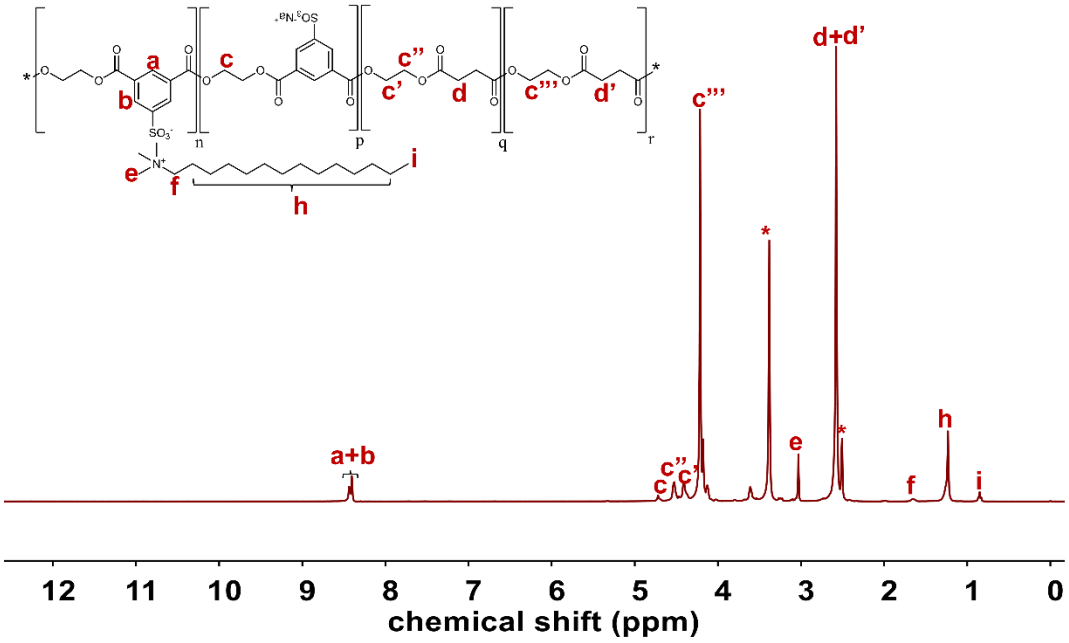

Figure S48. ^{1}H NMR spectrum of PESSIPA0.1-0.5%

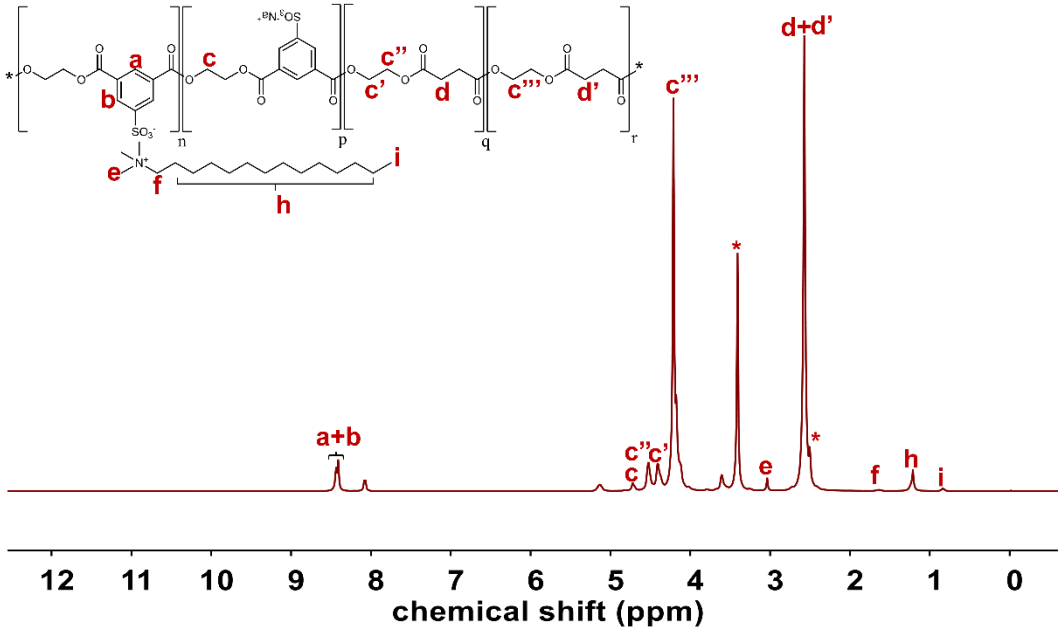

Figure S49. ^{1}H NMR spectrum of PESSIPA0.1-1%

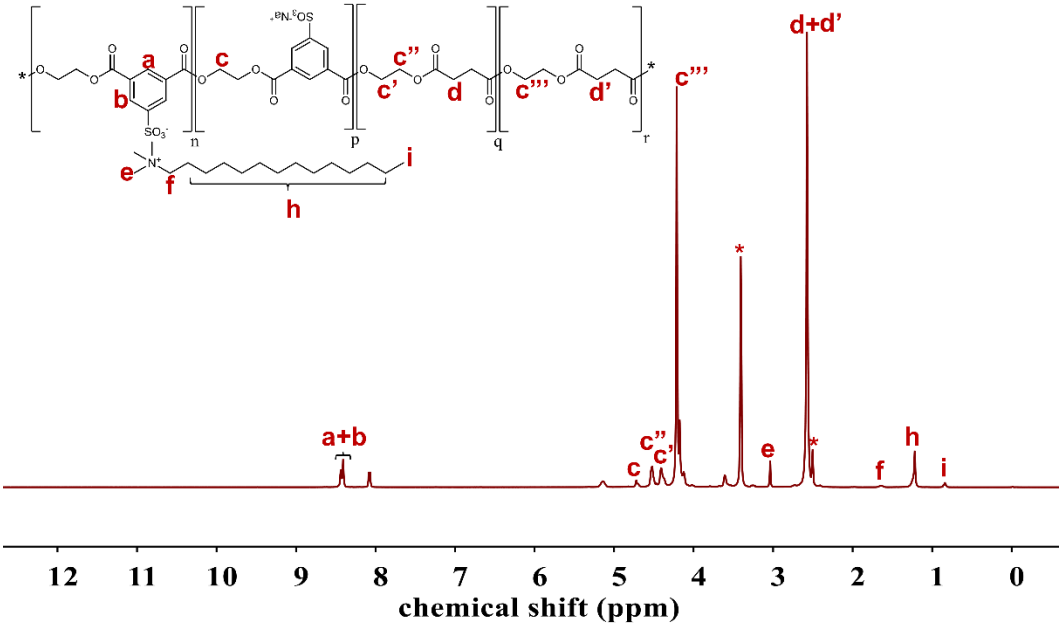

Figure S50. ^{1}H NMR spectrum of PESSIPA0.1-2%

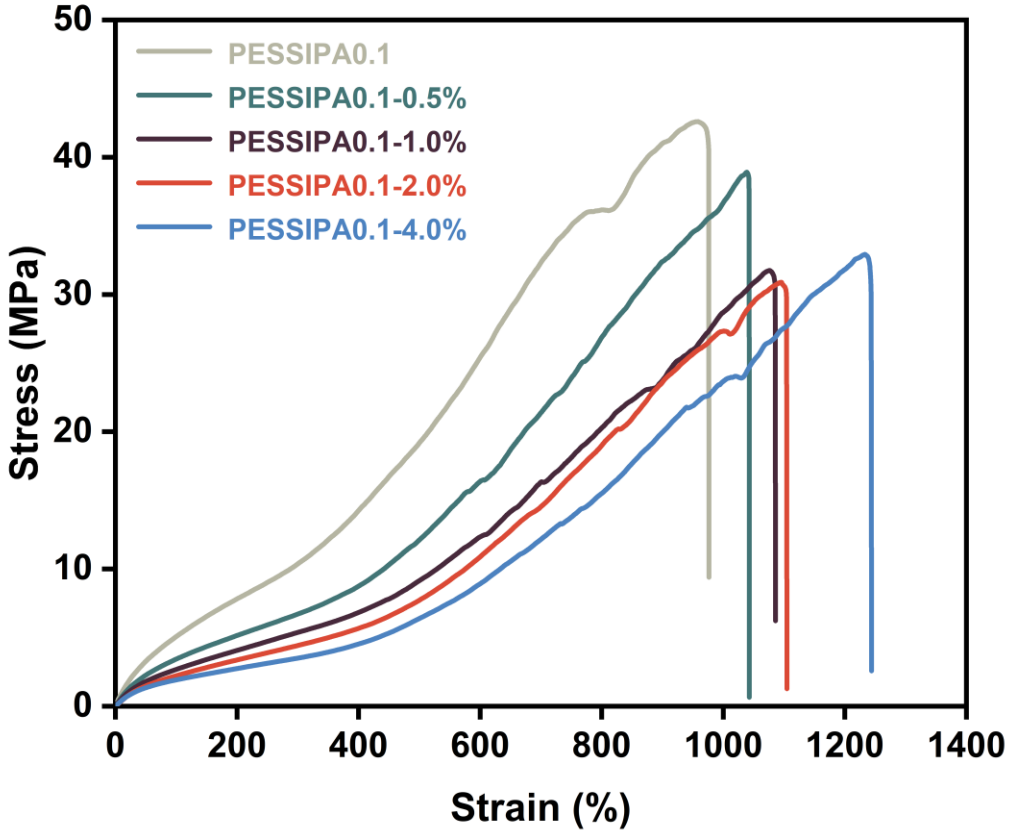

Figure S51. Tensile properties of PESSIPA0.1 containing antibacterial monomer concentrations ranging from 0.5% to 4.0%, compared to PESSIPA0.1 without antibacterial additive.

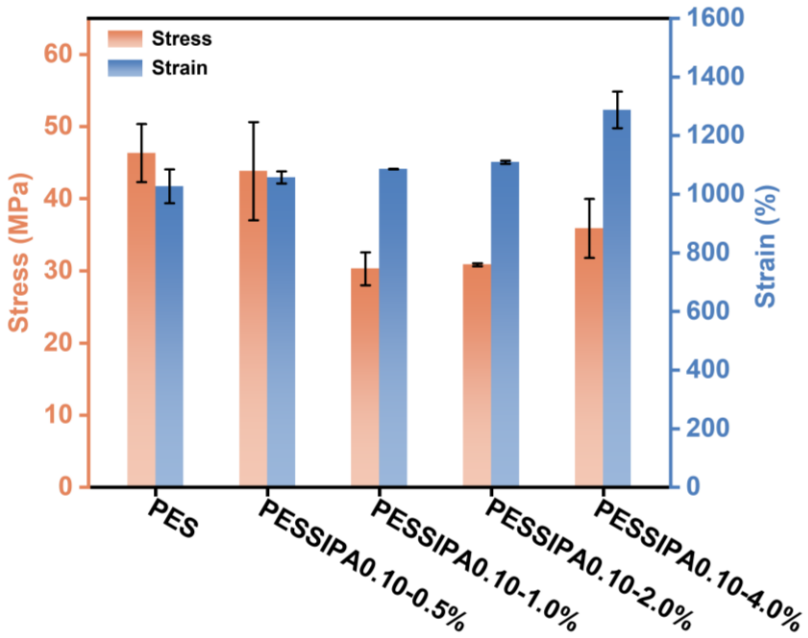

Figure S52. Tensile properties of PESSIPA0.1 containing antibacterial monomer concentrations ranging from 0.5% to 4.0%, compared to PESSIPA0.1 without antibacterial additive. Error bars represent standard deviation, n = 5.

6. Structure information of calculate process

Back-biting：

Reactant

C	-1.22422	1.06631	-0.33682
H	-2.03608	1.78071	-0.20668
H	-0.89365	1.13531	-1.37799
C	-1.82207	-0.33026	-0.18833
O	-2.95078	-0.57231	-0.49284
O	-0.99994	-1.32824	0.18106
H	-0.30142	-1.08475	0.80433
C	-0.05518	1.41879	0.59647
H	-0.3778	1.42363	1.63809
H	0.31407	2.41208	0.33697
C	2.73435	-0.48745	-0.87958
H	3.45419	-0.52498	-0.06338
H	2.2254	-1.44814	-0.96084
H	3.21853	-0.22482	-1.81527
C	1.08073	0.43033	0.48526
O	1.29479	-0.44118	1.29787
O	1.76796	0.54884	-0.64097

TS1

C	-1.33018	1.10157	-0.37416
H	-2.14011	1.80557	-0.18776

Esterification

Reactant

C	0.18176	-0.72185	0.9887
H	0.30601	0.2784	1.40569
H	0.65441	-1.44214	1.65223
C	0.83889	-0.85658	-0.3675
O	1.27929	-1.90089	-0.77815
O	0.73453	0.21228	-1.17677
H	0.15256	0.87661	-0.77485
C	-1.29073	-1.06465	0.78249
H	-1.77579	-1.38269	1.70754
H	-1.39391	-1.90018	0.08283
C	-4.21978	0.84144	-0.3521
H	-5.22379	0.42691	-0.35311
H	-4.16554	1.72179	0.28812
H	-3.9111	1.11049	-1.36206
C	-2.08247	0.09575	0.23779
O	-1.6289	1.17033	-0.08398
O	-3.37646	-0.19428	0.16138
C	3.02838	1.93829	0.53819
C	3.43821	0.69054	-0.21031
H	3.56435	2.81168	0.16337

H	-1.00609	1.22759	-1.41108
C	-1.81485	-0.35691	-0.19139
O	-2.96754	-0.63929	-0.4392
O	-0.85996	-1.1312	0.19431
H	0.28459	-1.02301	1.355
C	-0.15706	1.36151	0.58069
H	-0.49343	1.32101	1.61707
H	0.30433	2.33442	0.39126
C	2.68172	-0.53606	-0.85985
H	3.40525	-0.58159	-0.04918
H	2.15955	-1.48555	-0.96527
H	3.14861	-0.23189	-1.79064
C	0.91221	0.33369	0.41139
O	1.19617	-0.57644	1.28147
O	1.70462	0.49826	-0.58153

Intermediate

C	-1.3692	-0.72063	0.97047
H	-2.28132	-1.31357	1.0126
H	-1.28243	-0.15503	1.9014
C	-1.45954	0.27961	-0.16978
O	-2.37346	0.97024	-0.48814
O	-0.26762	0.30339	-0.83487
H	1.97035	-0.39628	-1.57918
H	1.95742	2.12223	0.42894
H	3.25235	1.81724	1.59973
H	3.12259	0.73429	-1.25793
H	4.52581	0.56543	-0.17629
O	2.81238	-0.39036	0.44893
H	3.046	-1.21783	0.01654

TS1

C	0.19477	-0.69638	1.0185
H	0.26631	0.28932	1.48351
H	0.64678	-1.42468	1.68932
C	1.00931	-0.73149	-0.26172
O	1.39511	-1.88057	-0.73497
O	0.72897	0.21691	-1.17161
H	0.12468	0.87706	-0.79348
C	-1.26499	-1.06547	0.75409
H	-1.75314	-1.41984	1.66446
H	-1.33477	-1.88393	0.03003
C	-4.21779	0.84014	-0.35071
H	-5.22106	0.42385	-0.35081
H	-4.16425	1.72082	0.28899
H	-3.90989	1.10864	-1.36104
C	-2.07646	0.09367	0.23199
O	-1.62781	1.17201	-0.08572

C	-0.09783	-1.50388	0.65486	O	-3.37181	-0.19545	0.1629
H	-0.29938	-2.35393	0.00262	C	3.0218	1.91628	0.5418
H	0.46227	-1.83085	1.52779	C	3.3648	0.6423	-0.20876
C	1.59795	1.69153	0.38783	H	3.60062	2.75769	0.15542
H	0.67063	2.26888	0.39286	H	1.96206	2.15696	0.42927
H	2.2952	2.09796	1.11716	H	3.23995	1.79939	1.60484
H	2.04282	1.76353	-0.60573	H	3.141	0.74365	-1.27592
C	0.70185	-0.47776	-0.13082	H	4.42609	0.40355	-0.10083
O	1.53826	-1.07931	-1.03914	O	2.63098	-0.44589	0.33487
O	1.37042	0.34412	0.77617	H	2.48233	-1.46671	-0.28592

TS2 **Intermediate**

C	-1.38912	-0.65222	0.97926	C	0.14085	0.50991	1.30929
H	-2.33371	-1.17409	1.11829	H	-0.26669	1.51201	1.46242
H	-1.20242	-0.04256	1.86789	H	0.74666	0.25836	2.17963
C	-1.48994	0.28981	-0.20653	C	1.11171	0.56503	0.12704
O	-2.3771	1.01491	-0.51363	O	0.55426	1.04834	-1.05319
O	-0.32803	0.2139	-0.93948	O	2.18592	1.41876	0.43841
H	2.16175	-0.23814	-0.24159	H	2.14643	2.14637	-0.18754
C	-0.19147	-1.52436	0.62848	C	-0.97921	-0.51593	1.15366
H	-0.48352	-2.41396	0.06586	H	-1.43827	-0.74159	2.11978
H	0.43294	-1.82179	1.46693	H	-0.58619	-1.45961	0.76754
C	1.4316	1.75292	0.4861	C	-4.15152	-0.58828	-0.72127
H	0.48896	2.06024	0.94315	H	-4.84782	-1.42106	-0.68031

H	2.25856	2.21578	1.02366	H	-4.62365	0.32982	-0.37234
H	1.44174	2.05715	-0.56217	H	-3.78359	-0.44064	-1.73641
C	0.58534	-0.64834	-0.33146	C	-2.08762	-0.0569	0.24161
O	1.57887	-1.06099	-1.03388	O	-2.11355	1.00049	-0.34818
O	1.57092	0.3385	0.60985	O	-3.06965	-0.94829	0.14611
Product				C	3.98603	-1.05085	-0.08642
C	-1.27869	-0.63008	1.02434	C	2.70336	-0.91581	-0.88981
H	-2.24283	-1.06828	1.27528	H	4.82805	-1.25944	-0.7514
H	-0.94739	-0.00905	1.86006	H	4.18469	-0.13312	0.46569
C	-1.429	0.28086	-0.17464	H	3.89533	-1.87566	0.6232
O	-2.27864	1.07154	-0.4151	H	2.75951	-0.0877	-1.60072
O	-0.36376	0.08305	-1.02903	H	2.50237	-1.82675	-1.45745
H	2.45783	0.26584	0.71266	O	1.57975	-0.73806	-0.02758
C	-0.19697	-1.61467	0.60072	H	-0.39223	1.21353	-0.93628
H	-0.60627	-2.57262	0.27093	**TS2**			
H	0.56593	-1.79997	1.35205	C	0.11481	0.4945	1.36188
C	1.52628	1.97921	0.57971	H	-0.26833	1.51132	1.4588
H	0.58401	2.37026	0.96508	H	0.65025	0.2638	2.28655
H	2.33522	2.63776	0.90564	C	1.19606	0.50172	0.29788
H	1.47692	1.96616	-0.51214	O	0.52985	1.19581	-1.11542
C	0.44013	-0.95111	-0.59938	O	2.10372	1.44662	0.34681
O	1.44595	-1.22668	-1.16504	H	1.40749	1.83599	-0.63431
O	1.67857	0.66787	1.10907	C	-1.01165	-0.5112	1.16163

Transesterification

Reactant

C	-1.49986	-1.08768	0.2056
H	-1.08813	-1.39543	-0.75974
H	-1.81206	-1.98481	0.73721
C	-2.76705	-0.27239	-0.02598
O	-3.85493	-0.68175	0.26841
O	-2.60843	0.93265	-0.57608
H	-1.66865	1.10815	-0.78972
C	-0.42197	-0.35968	1.01391
H	0.25544	-1.07027	1.48556
H	-0.87938	0.22015	1.82486
C	2.14109	2.17985	0.4285
H	2.92194	2.40591	1.14989
H	2.57226	2.00856	-0.55948
H	1.42516	2.99844	0.36138
C	0.39593	0.63899	0.23823
O	0.00985	1.24341	-0.75193
O	1.49403	1.00106	0.91277
C	2.79157	-2.01111	0.35651
C	2.70236	-1.0449	-0.80102
H	3.8083	-2.39458	0.45278
H	2.52071	-1.51936	1.29181
H	-1.4951	-0.74621	2.11342
H	-0.62749	-1.45663	0.77145
C	-4.17224	-0.5644	-0.72107
H	-4.86808	-1.39747	-0.67884
H	-4.64364	0.35271	-0.36804
H	-3.81015	-0.41388	-1.73803
C	-2.1028	-0.03164	0.23776
O	-2.12622	1.028	-0.34342
O	-3.08669	-0.92466	0.14017
C	3.9732	-1.02802	-0.07306
C	2.69431	-0.90945	-0.87756
H	4.8155	-1.21655	-0.74276
H	4.15652	-0.10451	0.47534
H	3.9023	-1.85776	0.63282
H	2.7307	-0.06868	-1.57086
H	2.49163	-1.81955	-1.44283
O	1.55343	-0.75703	-0.01566
H	-0.38433	1.49835	-0.98725

Product

C	0.14791	0.47947	1.38637
H	-0.22685	1.50309	1.39694
H	0.56677	0.29263	2.38082
C	1.37092	0.44924	0.48844

H	2.11698	-2.85227	0.18547	O	0.42184	1.23341	-1.30537
H	3.26252	-0.12874	-0.58455	O	2.16527	1.35974	0.4296
H	3.11184	-1.49172	-1.71204	H	0.95783	2.02353	-1.19786
O	1.33398	-0.7575	-0.99838	C	-0.97719	-0.52782	1.1488
H	1.20484	-0.19003	-1.7657	H	-1.46546	-0.77519	2.0954
TS1				H	-0.59167	-1.46884	0.75069
C	-1.50185	-1.09326	0.20968	C	-4.14848	-0.58499	-0.72216
H	-1.10047	-1.40863	-0.75787	H	-4.84422	-1.41822	-0.67887
H	-1.82278	-1.98787	0.73976	H	-4.62013	0.3324	-0.37014
C	-2.76496	-0.27137	-0.02514	H	-3.78742	-0.43551	-1.7397
O	-3.85383	-0.68024	0.26739	C	-2.07566	-0.04987	0.23124
O	-2.60119	0.93372	-0.5743	O	-2.11018	1.00854	-0.34852
H	-1.65811	1.10846	-0.78225	O	-3.06208	-0.9447	0.13884
C	-0.41211	-0.37009	1.01224	C	3.99878	-1.05079	-0.07498
H	0.17982	-1.08454	1.58552	C	2.71774	-0.92593	-0.87755
H	-0.85153	0.32611	1.73344	H	4.83774	-1.24244	-0.74757
C	2.13539	2.17655	0.42678	H	4.1952	-0.13081	0.47384
H	2.90884	2.424	1.14991	H	3.92756	-1.88175	0.62958
H	2.58146	2.0032	-0.55432	H	2.75147	-0.07789	-1.5635
H	1.4096	2.98444	0.34619	H	2.51179	-1.83326	-1.44497
C	0.53823	0.44615	0.16667	O	1.57484	-0.77055	-0.02489
O	0.06494	1.16069	-0.84588	H	-0.49877	1.49839	-1.18701
O	1.50795	0.99526	0.93417	**1-mer**			

C	2.77398	-2.00014	0.347	S	-0.43974	0.16244	0.00005
C	2.6296	-0.99293	-0.77599	O	-1.20107	1.42036	-0.00006
H	3.8	-2.37035	0.38628	O	0.43853	-0.05787	-1.221
H	2.54279	-1.5374	1.30775	O	0.43835	-0.05796	1.22115
H	2.10409	-2.84642	0.1852	Na	2.27453	-0.14613	-0.00003
H	3.2544	-0.11439	-0.59462	C	-1.63396	-1.1865	-0.00011
H	2.90761	-1.42607	-1.73859	H	-2.24594	-1.0875	0.89715
O	1.25848	-0.60208	-0.89892	H	-2.24611	-1.08708	-0.89722
H	0.79141	0.31014	-1.47819	H	-1.09475	-2.13418	-0.0004

Intermediate **2-mer**

C	-1.5017	-1.09142	0.19632	S	-2.26953	0.00021	-0.10131
H	-1.13148	-1.42548	-0.77867	O	-2.13255	1.26643	-0.88541
H	-1.81088	-1.97845	0.74578	O	-2.13103	-1.26532	-0.88633
C	-2.77436	-0.27794	-0.01922	O	-1.27398	0.00022	1.04157
O	-3.85973	-0.69548	0.26887	Na	0.	-1.72964	-0.00008
O	-2.63427	0.93578	-0.56396	S	2.26953	0.00021	0.10133
H	-1.69566	1.14783	-0.71293	O	2.131	-1.26534	0.88633
C	-0.38101	-0.35997	0.94847	O	1.27404	0.00022	-1.0416
H	0.17835	-1.06486	1.56571	O	2.13249	1.2664	0.88545
H	-0.78369	0.40209	1.62028	Na	0.	1.72899	-0.00007
C	2.14854	2.15955	0.41183	C	3.91573	-0.00106	-0.61349
H	2.91791	2.40735	1.14053	H	4.0216	0.89726	-1.22206
H	2.61351	2.01383	-0.5681	H	4.6334	-0.00107	0.2076

H	1.42204	2.96972	0.34533	H	4.02067	-0.89997	-1.22132
C	0.64349	0.32403	0.0485	C	-3.9157	-0.00109	0.6136
O	-0.00068	1.24166	-0.81178	H	-4.02154	0.89721	1.22221
O	1.53456	0.96961	0.89143	H	-4.63341	-0.00108	-0.20745
C	2.79259	-2.02578	0.39478	H	-4.0206	-0.90003	1.22141
C	2.61152	-0.98445	-0.68946	**3-mer**			
H	3.82196	-2.39087	0.39216	S	0.24155	2.32607	0.14294
H	2.58466	-1.59963	1.37808	O	-0.78461	3.3745	-0.16175
H	2.12433	-2.87176	0.22278	O	0.43885	2.05591	1.594
H	3.24868	-0.11712	-0.5019	O	-0.16316	1.0472	-0.58377
H	2.87479	-1.39439	-1.66555	Na	0.1412	-0.19612	1.74087
O	1.25187	-0.5808	-0.84711	S	-2.68874	-1.19308	0.05147
H	0.34952	1.08064	-1.69515	O	-1.89767	-1.03602	1.31129
TS2				O	-3.47996	0.03745	-0.29167
C	-1.59889	-1.48648	0.06497	O	-1.86016	-1.67034	-1.10239
H	-1.80464	-1.80103	-0.96116	Na	-2.37416	1.85702	-0.8002
H	-1.89872	-2.27725	0.7549	S	2.80776	-1.06755	-0.07898
C	-2.45115	-0.25464	0.4028	O	1.54009	-1.5294	0.62275
O	-2.92574	-0.04764	1.50632	O	2.548	-1.01223	-1.5568
O	-2.66384	0.57358	-0.65663	O	3.3681	0.17094	0.50671
H	-1.98208	0.35779	-1.37551	Na	0.26632	-1.05246	-1.36917
C	-0.08438	-1.256	0.22041	C	1.8117	2.84667	-0.53393
H	0.42095	-2.18874	-0.04845	H	2.08377	3.77923	-0.03772

H	0.15405	-1.01503	1.25922	H	2.53371	2.05504	-0.31849
C	1.07182	2.16162	0.62249	H	1.68291	2.99746	-1.60609
H	1.29502	1.89614	1.65701	C	4.0103	-2.37701	0.18428
H	1.96221	2.06869	-0.0025	H	4.926	-2.09499	-0.33666
H	0.67499	3.1769	0.58495	H	4.18698	-2.46259	1.25694
C	0.41883	-0.13874	-0.68494	H	3.60223	-3.30369	-0.21999
O	-0.34711	0.26275	-1.74028	C	-3.89802	-2.47875	0.37104
O	0.02564	1.2709	0.12231	H	-3.35685	-3.3916	0.62164
C	3.08027	-0.41847	1.16882	H	-4.52163	-2.15413	1.20442
C	2.75003	-0.91344	-0.24137	H	-4.49286	-2.614	-0.53263
H	3.82119	-1.0859	1.61937	**4-mer**			
H	3.4978	0.59026	1.13137	S	0.69974	0.77278	1.96043
H	2.19231	-0.4102	1.80687	O	-0.23172	1.73033	2.66272
H	3.63253	-0.8689	-0.88075	O	-0.06493	-0.34915	1.34059
H	2.39537	-1.94638	-0.21459	O	1.53052	1.55197	0.96875
O	1.77753	-0.0627	-0.94025	Na	-0.24775	-1.42276	-0.68875
H	-0.41201	1.36547	-0.98137	S	-0.84704	2.0997	-1.43873
Product				O	-0.20584	0.779	-1.70844
C	1.57523	-1.51499	-0.1419	O	-1.62371	2.1683	-0.14743
H	1.87163	-1.88135	0.84286	O	0.16561	3.212	-1.45271
H	1.90165	-2.23292	-0.89357	Na	0.08194	3.363	0.95135
C	2.29406	-0.2126	-0.46632	S	3.29334	-1.46935	-0.51806
O	2.63491	0.08698	-1.57132	O	1.92796	-1.42974	-1.17872

O	2.55481	0.59098	0.5867
H	2.05121	0.27595	1.35485
C	0.05154	-1.39769	-0.21242
H	-0.37008	-2.40759	-0.18501
H	-0.25142	-0.93924	-1.15631
C	-1.10782	2.52775	-0.38059
H	-1.61688	2.43528	-1.3409
H	-1.81445	2.30149	0.42524
H	-0.76198	3.55871	-0.27808
C	-0.53015	-0.59648	0.93668
O	0.14239	-0.1945	1.85387
O	-0.02922	1.61138	-0.37677
C	-2.99482	-0.14117	-1.2222
C	-2.74695	-0.98298	0.01528
H	-3.67551	-0.67476	-1.88901
H	-3.4547	0.809	-0.94994
H	-2.07074	0.06683	-1.76317
H	-3.67031	-1.10713	0.58081
H	-2.38614	-1.97811	-0.24729
O	-1.84756	-0.35815	0.94508
H	0.68009	1.93183	0.19655

O	3.99285	-0.17112	-0.80244
O	3.24773	-1.85713	0.90967
Na	2.03889	0.98317	-1.18464
S	-3.00614	-2.01133	0.08642
O	-3.38337	-1.57537	1.46892
O	-2.66694	-0.79912	-0.75248
O	-1.90544	-3.01505	0.01029
Na	-2.2368	0.46848	1.25885
C	-4.46479	-2.77357	-0.63433
H	-4.22325	-3.06609	-1.65668
H	-4.71581	-3.64696	-0.03127
H	-5.275	-2.04403	-0.61587
C	4.20922	-2.75235	-1.38375
H	5.21588	-2.78218	-0.96517
H	3.69527	-3.70033	-1.22074
H	4.23549	-2.49847	-2.44379
C	1.83208	0.04694	3.13188
H	1.23968	-0.4989	3.867
H	2.47635	-0.62575	2.5574
H	2.39924	0.85347	3.59736
C	-2.03772	2.35795	-2.74916
H	-1.50311	2.34609	-3.69938
H	-2.74909	1.53258	-2.68817
H	-2.52753	3.31786	-2.58415

7. Tables

Table S1. Synthesis of the PESSIPAs via melt polycondensation

Entry	Samples[b]	SA:EG:NaSIPA[c]		M_n	M_w	PDI
		Feed	^{1}H NMR	(kDa)[d]	(kDa)[d]	
1	PES	1.07:1.00:0.00	1.00:1.00:0.00	43.6	130	2.98
2	PESSIPA0.05	1.02:1.00:0.05	0.95:0.99:0.05	30.5	49.2	1.61
3	PESSIPA0.1	0.97:1.00:0.10	0.89:0.99:0.10	36.1	61.0	1.68
4	PESSIPA0.15	0.92:1.00:0.15	0.83:0.98:0.15	23.9	35.8	1.50
5	PESSIPA0.2	0.87:1.00:0.20	0.80:0.99:0.20	22.9	40.2	1.76
6	PESSIPA0.25	0.82:1.00:0.25	0.74:0.99:0.25	14.4	18.8	1.31

[a]Conditions: The first stage was conducted at 130-180 ℃ in the presence of a constant argon flow. The second stage was performed under 240 ℃ and high vacuum (<100 Pa). [b]The starting monomers were SA, EG and/or NaSIPA. [c]Molar ratio; The ratios in product were determined by ^{1}H NMR. [d]Measured by ultra-high performance polymer chromatography-multi-angle laser light scattering detector-differential detector (APC-MALLS-RID) detection technology.

Table S2. Summary of T_g, T_m and $T_{d,10\%}$ of PESSIPAs.

Entry	Samples	T_g (°C) [a]	T_m (°C) [b]	$T_{d,10\%}$ (°C) [c]
1	PES	-8.8	102.7	349
2	PESSIPA0.05	3.3	n.d.	357
3	PESSIPA0.1	0.8	n.d.	344
4	PESSIPA0.15	1.3	n.d.	327
5	PESSIPA0.20	6.5	n.d.	330
6	PESSIPA0.25	11.9	n.d.	307

[a]Determined by the vertex of the loss modulus curves (E''). [b]Determined by the DSC curves. [c]Determined by the TGA curves. n.d. = not determined.

8. References

[1] K.-C. Hoang, M. Tseng, W.-J. Shu, Degradation of polyethylene succinate (PES) by a new thermophilic Microbispora strain, Biodegradation 18(3) (2007) 333-342. https://doi.org/10.1007/s10532-006-9067-5.
[2] Y. Ikada, H. Tsuji, Biodegradable polyesters for medical and ecological applications, Macromol. Rapid Commun. 21(3) (2000) 117-132. https://doi.org/10.1002/(SICI)1521-3927(20000201)21:3<117::AID-MARC117>3.0.CO;2-X.
[3] M. Okada, Chemical syntheses of biodegradable polymers, Prog. Polym. Sci. 27(1) (2002) 87-133. https://doi.org/10.1016/S0079-6700(01)00039-9.
[4] G.-X. Wang, D. Huang, J.-H. Ji, C. Völker, F.R. Wurm, Seawater-Degradable Polymers—Fighting the Marine Plastic Pollution, Adv. Sci. 8(1) (2021) 2001121. https://doi.org/10.1002/advs.202001121.
[5] M. Deroiné, A. Le Duigou, Y.-M. Corre, P.-Y. Le Gac, P. Davies, G. César, S. Bruzaud, Accelerated ageing of polylactide in aqueous environments: Comparative study between distilled water and seawater, Polym. Degrad. Stabil. 108 (2014) 319-329. https://doi.org/10.1016/j.polymdegradstab.2014.01.020.
[6] T. Lu, Q. Chen, Shermo: A general code for calculating molecular thermochemistry properties, Comput. Theor. Chem. 1200 (2021) 113249. https://doi.org/10.1016/j.comptc.2021.113249.